Evaluating the Effectiveness of GANs in Augmenting Heterogeneous Datasets for Healthcare Applications

A report submitted for the completion of the mini project

BACHELOR OF TECHNOLOGY

in

INFORMATION TECHNOLOGY

Submitted by

Rishu Raj (IIT2022134)
Aditya Dwivedi (IIT2022147)
Vikas Singh (IIT2022151)
Prachi Kumari (IIT2022206)
Owaish Jamal (IIB2022037)

Under the supervision of

Dr. Manish Kumar

to the

Department of Information Technology

,

Indian Institute of Information Technology, Allahabad

December 4, 2024

भारतीय सूचना प्रौद्योगिकी संस्थान इलाहाबाद
Indian Institute of Information Technology Allahabad
An Institute of National Importance by Act of Parliament
Deoghat Jhalwa, Prayagraj 211015 (U.P.) India
Ph: 0532-2922025, 2922067; Web: www.iiita.ac.in; Email: contact@iiita.ac.in

Supervisor's Certification

It is certified that the work contained in this report titled **"Evaluating the Effectiveness of Generative Adversarial Networks (GANs) in Augmenting Heterogeneous Datasets for Healthcare Applications"** by Rishu Raj (IIT2022134), Aditya Dwivedi (IIT2022147), Vikas Singh (IIT2022151), Prachi Kumari (IIT2022206), Owaish Jamal (IIB2022037), has been carried out under my/our supervision and that this work has not been submitted elsewhere for a degree.

Dr. Manish Kumar
Department of Information Technology
IIIT Allahabad

भारतीय सूचना प्रौद्योगिकी संस्थान इलाहाबाद
Indian Institute of Information Technology Allahabad
An Institute of National Importance by Act of Parliament
Deoghat Jhalwa, Prayagraj 211015 (U.P.) India
Ph: 0532-2922025, 2922067; Web: www.iiita.ac.in; Email: contact@iiita.ac.in

CANDIDATE DECLARATION

We, **Rishu Raj (IIT2022134), Aditya Dwivedi (IIT2022147), Vikas Singh (IIT2022151), Prachi Kumari (IIT2022206), Owaish Jamal (IIB2022037)**, certify that this thesis work titled **"Evaluating the Effectiveness of Generative Adversarial Networks (GANs) in Augmenting Heterogeneous Datasets for Healthcare Applications"** is submitted by us towards partial fulfillment of the requirement of the Degree of Master of Technology in the Department of Information Technology, Indian Institute of Information Technology, Allahabad.

We understand that plagiarism includes:

1. Reproducing someone else's work (fully or partially) or ideas and claiming it as one's own.
2. Reproducing someone else's work (verbatim copying or paraphrasing) without crediting.
3. Committing literary theft (copying some unique literary construct).

We have given due credit to the original authors/sources through proper citation for all the words, ideas, diagrams, graphics, computer programs, experiments, results, and websites that are not our original contributions. We have used quotation marks to identify verbatim sentences and given due credit to the original authors/sources.

We affirm that no portion of our work is plagiarized. In the event of a complaint of plagiarism, we shall be fully responsible. We understand that our supervisor may not be in a position to verify that this work is not plagiarized.

Date: _____

Rishu Raj (IIT2022134)
Aditya Dwivedi (IIT2022147)
Vikas Singh (IIT2022151)
Prachi Kumari (IIT2022206)
Owaish Jamal (IIB2022037)
Department of Information Technology
Indian Institute of Information Technology, Allahabad
Prayagraj - 211015, U.P.

Abstract

Generative Adversarial Networks (GANs) have emerged as powerful tools for data augmentation, especially in domains where acquiring large and diverse datasets is challenging. This study investigates the effectiveness of GANs and their advanced variants in augmenting heterogeneous datasets for healthcare applications, with a focus on medical imaging and sequential data. Specifically, we analyze the performance of five GAN variants: Classical GAN, Wasserstein GAN (WGAN), Deep Convolutional GAN (DCGAN), BiLSTM-DCGAN, and VAEGAN, using two types of datasets—X-ray images and ECG signals.

For X-ray images, the quality of GAN-generated synthetic samples was evaluated using metrics such as Fréchet Inception Distance (FID), Peak Signal-to-Noise Ratio (PSNR), and Structural Similarity Index Measure (SSIM). In contrast, ECG signal augmentation was assessed using Root Mean Square Error (RMSE), Dynamic Time Warping (DTW), and Mean Absolute Error (MAE). To ensure high-quality inputs for training, preprocessing steps such as normalization and noise removal were applied.

The results demonstrate that advanced GAN variants, such as DCGAN and BiLSTM-DCGAN, significantly outperform Classical GANs in generating realistic and clinically usable data. While WGAN provided superior stability during training, BiLSTM-DCGAN excelled in capturing sequential dependencies in ECG data. Similarly, VAEGAN demonstrated robust augmentation capabilities for complex X-ray images by leveraging its variational inference features.

This study offers valuable insights into the comparative strengths and limitations of various GAN architectures in addressing the challenges associated with heterogeneous data augmentation. Our findings suggest that carefully selected GAN variants can improve the diversity and quality of synthetic data, potentially enhancing the accuracy and generalizability of downstream healthcare applications, including disease diagnosis and treatment planning. Future work will focus on optimizing these architectures for broader applications and integrating them into real-world clinical workflows.

Acknowledgment

We would like to express our sincere gratitude to **Mr. Manish Kumar**, our esteemed supervisor and professor, for his invaluable guidance, support, and encouragement throughout the course of this project. His insights and expertise were instrumental in shaping the direction of our research and ensuring its successful completion.

We also extend our heartfelt thanks to **Mr. Shahanwaz**, **Mr. Ankit**, and **Mr. Shashank**, for their continuous support, timely feedback, and assistance during various stages of the project. Their constructive inputs and encouragement were essential in overcoming challenges and refining our work.

This project would not have been possible without the inspiration and mentorship provided by these individuals, and we are deeply grateful for their contributions.

Contents

Acknowledgment **2**

1 Introduction **7**
1.1 Background . . . 7
1.2 Problem Statement . . . 8
1.3 Objectives . . . 8
1.4 GAN . . . 9
1.5 Minimax Game in GANs . . . 9
1.6 Scope . . . 10
1.6.1 Chest X-ray Images . . . 10
1.6.2 ECG Signals . . . 10
1.7 Research Contribution . . . 11

2 Literature Review **12**
2.1 Overview of Generative Adversarial Networks (GANs) . . . 12
2.1.1 Architecture of GANs . . . 12
2.1.2 How the Training Works . . . 12
2.1.3 Loss Function of GANs . . . 13
2.1.4 Challenges in GANs . . . 14
2.2 GAN Variants . . . 14
2.2.1 Deep Convolutional GAN (DCGAN) . . . 15
2.2.2 Wasserstein GAN (WGAN) . . . 16
2.2.3 BiLSTM-DCGAN . . . 17
2.2.4 Variational Autoencoder GAN (VAEGAN) . . . 19
2.2.5 Comparison of GAN Variants . . . 20
2.3 Summary of GAN Variants . . . 20
2.3.1 Previous Applications of GANs in Healthcare . . . 21
2.3.2 Challenges in Data Augmentation . . . 22
2.3.3 Summary of Insights from Reviewed Papers . . . 23

3 Methodology **25**
3.1 Datasets . . . 25
3.1.1 X-ray Images . . . 25
3.1.2 ECG Signals . . . 27
3.2 GAN Models for Data Augmentation . . . 29
3.3 Evaluation Metrics . . . 30
3.3.1 FID (Fréchet Inception Distance) . . . 30
3.3.2 PSNR (Peak Signal-to-Noise Ratio) . . . 31
3.3.3 SSIM (Structural Similarity Index) . . . 31

3.3.4 RMSE (Root Mean Squared Error) 32
3.3.5 DTW (Dynamic Time Warping) 32
3.3.6 MAE (Mean Absolute Error) 33

4 Results and Discussion **34**
4.1 Quantitative Analysis 34
4.1.1 Frechet Inception Distance (FID) 34
4.1.2 Peak Signal-to-Noise Ratio (PSNR) 35
4.1.3 Structural Similarity Index Measure (SSIM) 36
4.2 Comparative Summary of Results 36
4.3 Discussion and Key Insights 36
4.4 Analysis of Loss Across GAN Variants 39
4.4.1 Classical GAN 39
4.4.2 DCGAN (Deep Convolutional GAN) 40
4.4.3 WGAN (Wasserstein GAN) 42
4.4.4 VAE-GAN (Variational Autoencoder-GAN) 44
4.4.5 BiLSTM-DCGAN 45
4.4.6 Final Conclusion for the X-ray Dataset 45
4.4.7 Recommendations and Future Directions 47
4.4.8 Overall Recommendation 47
4.5 Results for ECG Dataset 47
4.5.1 Quantitative Analysis 47
4.5.2 Comparison of Results Across GAN Variants 49
4.6 Conclusion for ECG Dataset 54
4.7 Comparative Analysis 55
4.7.1 GAN Variants Evaluated 55
4.7.2 Performance Comparison for ECG Dataset 55
4.7.3 Performance Comparison for X-ray Dataset 56
4.7.4 Insights and Observations 58

5 Conclusion and Future Work **59**
5.1 Conclusion 59
5.2 Limitations of the Study 62
5.3 Future Work 62

List of Figures

1.1 Basic GAN Architecture. 10

2.1 GAN Training Instability with JS Divergence 14
2.2 Mode Collapse Visualization 14
2.3 DC-GAN Architecture 15
2.4 WGAN Gradient Flow 16
2.5 BiLSTM-DC GAN Architecture 18
2.6 AE/VAE-DC GAN Architecture 19

3.1 Training sample after preprocessing. 27
3.2 Grayscaled X-Ray 28
3.3 Classification of Dataset. 29

4.1 Classical GAN metrices. 37
4.2 DCGAN metrices. 37
4.3 WGAN metrices. 37
4.4 BiLSTM DCGAN metrices. 38
4.5 VAE DCGAN metrices. 38
4.6 Classical GAN Loss. 40
4.7 Classical GAN Generated Images. 41
4.8 DCGAN Loss. 41
4.9 DCGAN Generated Images. 42
4.10 WGAN Loss. 42
4.11 WGAN Generated Images. 43
4.12 VAE DCGAN Loss. 44
4.13 VAE DCGAN Generated Images. 44
4.14 BiLSTM DCGAN Loss. 45
4.15 BiLSTM DCGAN Generated Images. 46
4.16 Classical GAN Generated ECG Signals. 50
4.17 VAE DCGAN Generated ECG signals. 50
4.18 WGAN Generated ECG signals. 51
4.19 Classical GAN error. 51
4.20 VAE DCGAN error. 52
4.21 WGAN error. 52
4.22 CLassical GAN Plots. 53
4.23 WGAN Plots. 53
4.24 VAE DCGAN Plots. 54

List of Tables

2.1 Comparison of Different GAN Variants in Healthcare Applications 24

4.1 Comparative Summary of Results for Different GAN Variants . 39
4.2 Quantitative Comparison of ECG Signal Generation for Different GAN Variants 49
4.3 Performance Comparison for ECG Dataset 55
4.4 Performance Comparison for X-ray Dataset 57

Chapter 1

Introduction

1.1 Background

The exponential growth of machine learning and deep learning in recent years has transformed numerous fields, particularly healthcare. However, one persistent challenge in developing high-performance models for healthcare applications is the scarcity of large, labeled datasets. This issue is compounded by the complexity and variability of medical data, which often come in heterogeneous forms, such as imaging data (e.g., chest X-rays, MRIs) and time-series data (e.g., ECG and EEG signals).

Data augmentation, a technique used to artificially expand training datasets, plays a crucial role in addressing this limitation. Traditional augmentation methods, such as geometric transformations, noise addition, and scaling, are widely used but have inherent limitations in generating realistic and diverse data, particularly for complex and domain-specific datasets like medical images and signals.

Generative Adversarial Networks (GANs), introduced by Ian Goodfellow in 2014, have emerged as a groundbreaking approach for synthetic data generation. GANs consist of two neural networks, a generator, and a discriminator, that compete in a zero-sum game to improve each other's performance. The result is a generator capable of producing high-quality synthetic data that mimics the underlying distribution of real-world datasets. The ability of GANs to create entirely new data points, as opposed to merely transforming existing ones, makes them particularly valuable for healthcare applications where data diversity and quality are paramount.

Healthcare presents unique challenges due to the heterogeneity of its datasets. For instance, chest X-ray images require maintaining spatial features for accurate diagnosis, while ECG signals demand temporal and morphological consistency. This heterogeneity necessitates a robust and adaptable data augmentation method. Despite the promise of GANs, their performance across diverse medical datasets has not been extensively explored, motivating the need for this study.

1.2 Problem Statement

The effective training of machine learning models in healthcare is often hindered by:

1. **Limited Dataset Availability:** Medical datasets are typically small due to privacy concerns, the cost of data collection, and the need for expert annotations.

2. **Class Imbalance:** Certain classes (e.g., normal vs. abnormal cases) are disproportionately represented, leading to biased model predictions.

3. **Heterogeneity of Data:** Healthcare data varies significantly across modalities, requiring augmentation methods that are generalizable yet tailored to specific data types.

Traditional data augmentation methods address some of these challenges but fail to generate the diverse and high-quality synthetic data required for robust model training. GANs offer a potential solution but need to be rigorously evaluated across different healthcare datasets and metrics. This study aims to bridge this gap by assessing the effectiveness of GANs and their variants in augmenting heterogeneous datasets, specifically chest X-ray images and ECG signals.

1.3 Objectives

The objectives of this research are as follows:

Primary Objectives

1. To explore and implement five variants of GANs: Classical GAN, Deep Convolutional GAN (DCGAN), Wasserstein GAN (WGAN), Bidirectional Long Short-Term Memory-DCGAN (BiLSTM-DCGAN), and Variational Autoencoder GAN (VAEGAN).

2. To evaluate the quality of synthetic data generated by these models for two distinct datasets: chest X-ray images and ECG signals.

Secondary Objectives

[label=.]To analyze the performance of GANs using quantitative metrics tailored to each dataset:

1.
   - **For X-ray Images:** Frechet Inception Distance (FID), Peak Signal-to-Noise Ratio (PSNR), and Structural Similarity Index Measure (SSIM).
   - **For ECG Signals:** Root Mean Square Error (RMSE), Dynamic Time Warping (DTW), and Mean Absolute Error (MAE).

2. To compare the strengths and limitations of the selected GAN variants in handling heterogeneous healthcare data.

3. To provide insights and recommendations for future research and practical applications of GANs in healthcare.

1.4 GAN

At its core, a GAN consists of two main components[1]:

- **Generator (G)**: The role of the generator is to create synthetic data from a noise vector. It takes random noise (z), sampled from a simple distribution (often a uniform or Gaussian distribution), and transforms it into data that resembles the real dataset. Mathematically, the generator function can be represented as:
$$\hat{x} = G(z)$$
where z is the input noise vector and $G(z)$ is the generated synthetic data (e.g., an image, signal, etc.).

- **Discriminator (D)**: The discriminator, on the other hand, is a classifier that takes an input (either real or generated data) and outputs a probability that the input is real (from the actual dataset) or fake (from the generator). Its goal is to maximize its ability to correctly classify real and fake data:
$$D(x) \quad probability$$
where x is either a real or generated sample.

GANs are trained in a minimax game, where:

- The generator tries to fool the discriminator by creating realistic data.
- The discriminator tries to correctly identify whether the data is real or generated.

1.5 Minimax Game in GANs

The training process for GANs can be mathematically formulated as a minimax game[1], with the following objective function $V(G, D)$:

$$\min_G \max_D V(D, G) = \mathbb{E}_{x \sim p_{data}(x)}[\log D(x)] + \mathbb{E}_{z \sim p_z(z)}[\log(1 - D(G(z)))]$$

Here:

- $D(x)$ is the discriminator's probability that real data x is indeed real.
- $D(G(z))$ is the discriminator's probability that generated data $G(z)$ is real.
- $G(z)$ is the data generated by the generator from noise z.
- $p_{data}(x)$ is the real data distribution.
- $p_z(z)$ is the noise distribution.

In simpler terms:

- The discriminator tries to maximize the log-probability of correctly classifying real data (the first term) and minimize the log-probability of incorrectly classifying generated data (the second term).
- The generator tries to minimize the second term by generating data that maximizes the discriminator's mistake, i.e., $\log(1 - D(G(z)))$.

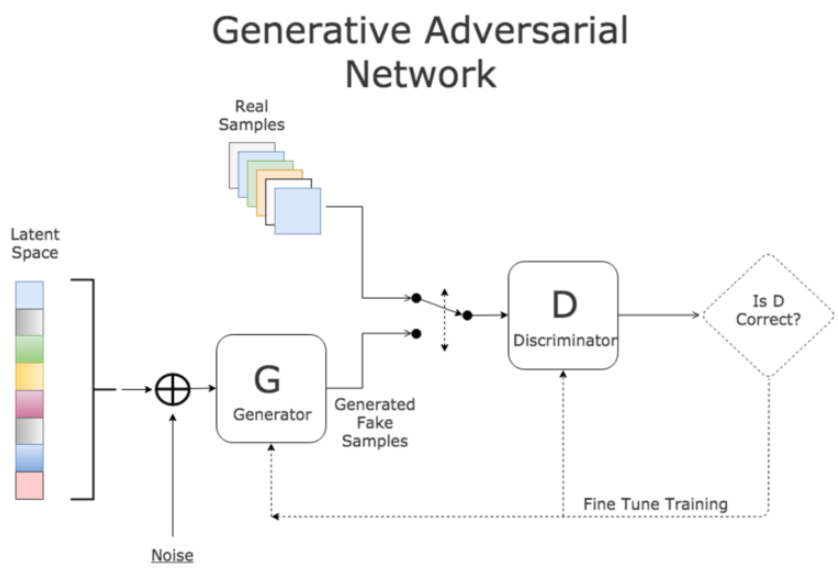

Figure 1.1: Basic GAN Architecture.

1.6 Scope

This project is specifically focused on the application of GANs to augment two distinct types of healthcare datasets:

1.6.1 Chest X-ray Images

- **Purpose:** X-ray imaging is a critical diagnostic tool for detecting pulmonary diseases, including pneumonia, tuberculosis, and COVID-19.
- **Preprocessing Steps:** Images are resized, normalized, and subjected to noise removal to ensure compatibility with GAN architectures.
- **Evaluation Metrics:** FID evaluates the similarity between real and generated image distributions, PSNR assesses the quality of reconstructed images, and SSIM quantifies the structural fidelity of generated images.

1.6.2 ECG Signals

- **Purpose:** Electrocardiograms (ECGs) are widely used to monitor cardiac health and diagnose arrhythmias and other cardiac conditions.

- **Preprocessing Steps:** Signals are filtered to remove noise, segmented into fixed-length windows, and standardized for GAN input.
- **Evaluation Metrics:** RMSE quantifies the error between real and generated signals, DTW measures temporal alignment, and MAE provides an average error metric.

By selecting these datasets, the project aims to explore the versatility and effectiveness of GANs across both spatial and temporal data modalities.

1.7 Research Contribution

This study contributes to the field of healthcare data augmentation by:

1. Providing a comprehensive evaluation of GAN variants for generating synthetic data in heterogeneous healthcare domains.
2. Establishing a benchmark for comparing GAN-generated data against traditional augmentation methods.
3. Offering insights into the practical challenges and considerations of using GANs for medical data augmentation.

Chapter 2

Literature Review

2.1 Overview of Generative Adversarial Networks (GANs)

Generative Adversarial Networks (GANs) represent a groundbreaking approach to generative modeling, introduced by Ian Goodfellow in 2014. GANs consist of two competing neural networks: the generator and the discriminator, engaged in a zero-sum game where the generator aims to produce realistic data, and the discriminator seeks to distinguish between real and generated data.

2.1.1 Architecture of GANs

The core architecture of GANs involves the following components[1]:

- **Generator (G)**: The generator is a neural network that learns to create synthetic data that resembles real data from a given distribution. It takes random noise as input and transforms it into synthetic data. Its goal is to fool the discriminator into classifying its outputs as real.
- **Discriminator (D)**: The discriminator is another neural network that evaluates whether a given input is real or generated by the generator. It is trained to assign a probability of realness to the input data, with a goal of distinguishing between true data points and fake ones generated by the generator.

The two networks are trained simultaneously, with the generator learning to produce more convincing fake data and the discriminator learning to become more adept at distinguishing between real and fake data. The training process can be understood as a minimax game, where the generator tries to minimize the discriminator's ability to distinguish real data from fake, and the discriminator tries to maximize its own ability to classify data correctly.

2.1.2 How the Training Works

The GAN training process alternates between two steps:

1. Discriminator Update

The discriminator is trained to maximize its ability to differentiate real data from fake data. This means adjusting its weights to increase the probability of correctly identifying real samples and minimizing the probability of being fooled by the generator's samples.

- The loss for the discriminator when trained on real data is $\log D(x)$.
- The loss for fake data is $\log(1 - D(G(z)))$.

The total discriminator loss can be written as:

$$L_D = -\left[\mathbb{E}_{x \sim p_{data}(x)}[\log D(x)] + \mathbb{E}_{z \sim p_z(z)}[\log(1 - D(G(z)))]\right]$$

2. Generator Update

The generator is trained to fool the discriminator, i.e., to minimize $\log(1 - D(G(z)))$, making its fake data look as real as possible. The generator's goal is to minimize the following loss:

$$L_G = -\mathbb{E}_{z \sim p_z(z)}[\log D(G(z))]$$

Each iteration of training involves adjusting the generator and discriminator's weights using backpropagation. The generator gradually gets better at generating realistic data, and the discriminator gets better at distinguishing fake from real data—until the generator becomes good enough to consistently fool the discriminator.

2.1.3 Loss Function of GANs

The original loss function used in GANs is based on the concept of Jensen-Shannon Divergence, which measures the difference between two probability distributions. In the context of GANs, it is represented as[1]:

$$\mathcal{L}_{GAN}(D, G) = \mathbb{E}_{x \sim p_{data}(x)}[\log D(x)] + \mathbb{E}_{z \sim p_z(z)}[\log(1 - D(G(z)))]$$

Where:

- $D(x)$ is the discriminator's output for real data x.
- $G(z)$ is the generated data from the generator given a random input z.
- $p_{data}(x)$ is the real data distribution.
- $p_z(z)$ is the noise distribution.

The objective of training is for the generator to learn to produce data such that $D(G(z)) \approx 1$ (i.e., fooling the discriminator), while the discriminator should aim to correctly classify real data as real and generated data as fake.

2.1.4 Challenges in GANs

- **Mode Collapse**: The generator may produce a limited variety of outputs, making the generated data appear similar despite different inputs.
- **Training Instability**: Due to the adversarial nature of the game, GANs can suffer from unstable training dynamics, requiring careful tuning of hyperparameters.

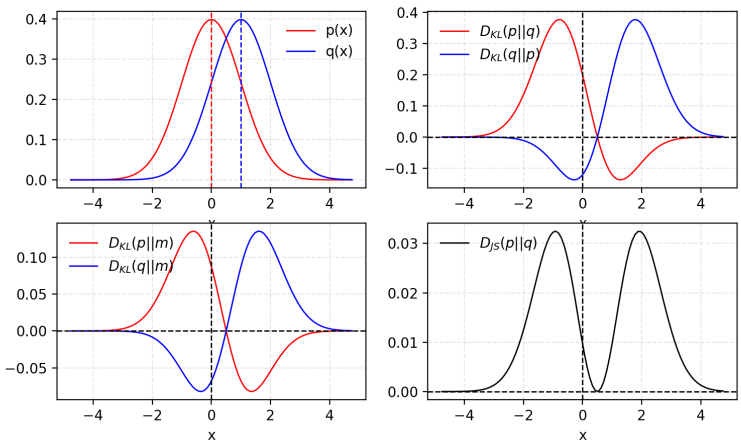

Figure 2.1: GAN Training Instability with JS Divergence

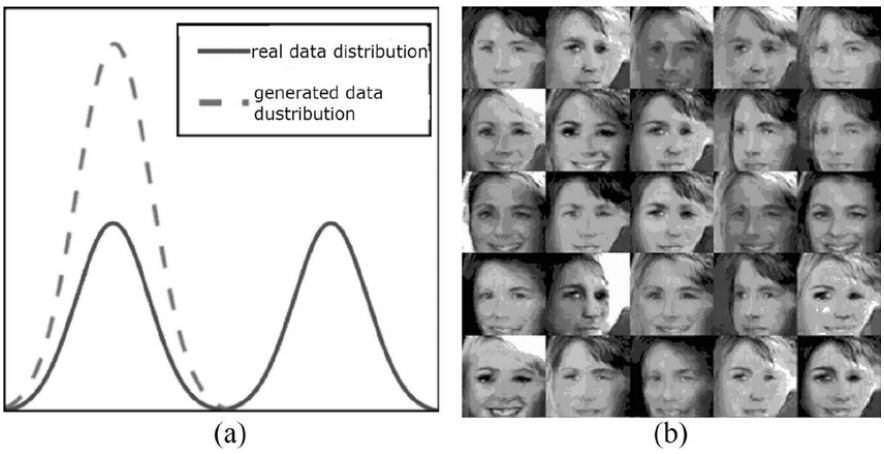

Figure 2.2: Mode Collapse Visualization

2.2 GAN Variants

While the classical GAN model laid the foundation for generative modeling, various enhancements have been proposed to address its limitations. Below, we discuss the most important GAN variants and their mathematical formulation, loss functions, and unique characteristics.

2.2.1 Deep Convolutional GAN (DCGAN)

Motivation

The classical GAN model was found to struggle with image data due to the high-dimensional nature of images. DCGAN[2], proposed by Radford et al. (2015), adapted the GAN architecture to handle image data by using convolutional layers instead of fully connected layers in both the generator and discriminator.

Architecture

- **Generator**: The generator in DCGAN uses transposed convolutional layers (also known as deconvolutions) to upsample random noise into an image. The generator typically uses a deep architecture to produce higher-dimensional images from the latent space.
- **Discriminator**: The discriminator uses standard convolutional layers to classify the input image as either real or fake.

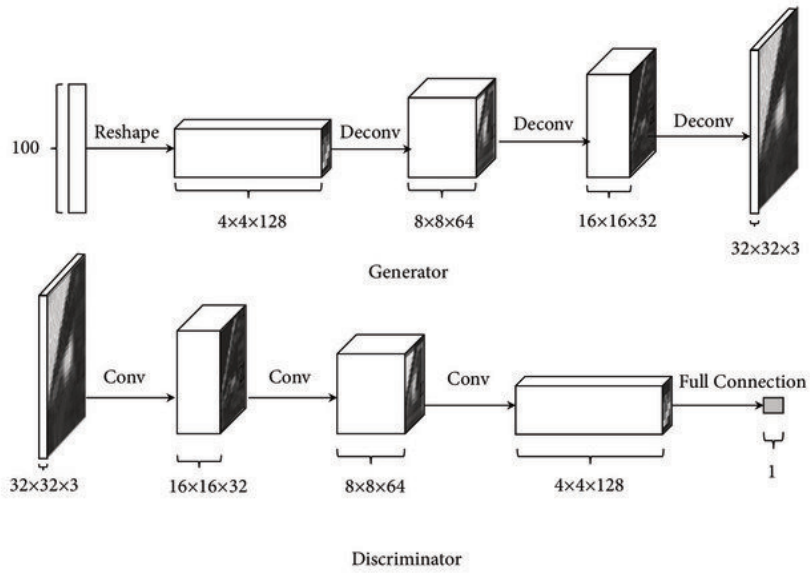

Figure 2.3: DC-GAN Architecture

Loss Function

The loss functions for DCGAN are as follows:

$$\mathcal{L}_D = -\mathbb{E}_{x\sim p_{data}(x)}[\log D(x)] - \mathbb{E}_{z\sim p_z(z)}[\log(1 - D(G(z)))]$$

$$\mathcal{L}_G = -\mathbb{E}_{z\sim p_z(z)}[\log D(G(z))]$$

Strengths

- Produces high-quality images, especially for high-dimensional data like medical images.
- Widely used for medical image generation, including chest X-rays and MRI scans.

Challenges

- Requires large amounts of labeled data for effective training.
- May still experience mode collapse or instability in training without careful regularization.

2.2.2 Wasserstein GAN (WGAN)

Motivation

A major limitation of classical GANs is instability during training, particularly due to the vanishing gradients problem when the discriminator becomes too confident. WGAN[2], introduced by Arjovsky et al. (2017), proposed a new loss function based on Wasserstein distance, a measure of the distance between probability distributions.

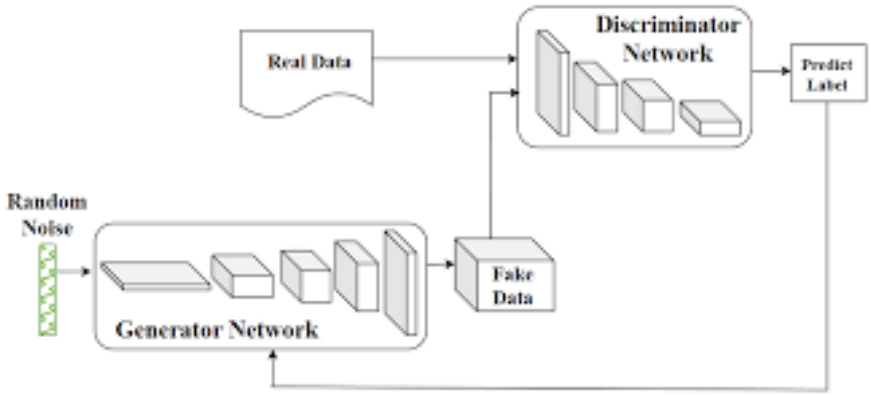

Figure 2.4: WGAN Gradient Flow

Loss Function

$$\mathcal{L}_D = \mathbb{E}_{x\sim p_{data}(x)}[D(x)] - \mathbb{E}_{z\sim p_z(z)}[D(G(z))]$$

$$\mathcal{L}_G = -\mathbb{E}_{z\sim p_z(z)}[D(G(z))]$$

Strengths

- More stable training.
- Less prone to mode collapse.

Challenges

- Weight clipping may lead to suboptimal performance if not tuned properly.
- Requires additional techniques like gradient penalty for improved performance (WGAN-GP).

2.2.3 BiLSTM-DCGAN

Motivation

BiLSTM-DCGAN extends the classical DCGAN architecture by incorporating Bidirectional Long Short-Term Memory (BiLSTM) networks, which are effective for sequential data modeling[2]. This architecture is particularly suited for datasets with temporal dependencies, such as ECG signals in healthcare applications.

Architecture

- **Generator**: The generator combines BiLSTM layers with transposed convolutional layers. The BiLSTM layers capture temporal patterns in the input sequence, while the convolutional layers generate synthetic sequences with the learned patterns.
- **Discriminator**: The discriminator integrates standard convolutional layers with LSTM layers to evaluate the sequential coherence of the generated data.

Loss Function

The loss functions for BiLSTM-DCGAN follow the standard GAN structure:

$$\mathcal{L}_D = -\mathbb{E}_{x\sim p_{data}(x)}[\log D(x)] - \mathbb{E}_{z\sim p_z(z)}[\log(1 - D(G(z)))]$$

$$\mathcal{L}_G = -\mathbb{E}_{z\sim p_z(z)}[\log D(G(z))]$$

Strengths

- Effectively captures temporal dependencies in sequential data.
- Suitable for generating realistic synthetic time-series data, such as ECG signals.

Challenges

- Higher computational requirements due to the combination of LSTM and convolutional layers.
- Requires careful tuning to avoid overfitting on sequential patterns.

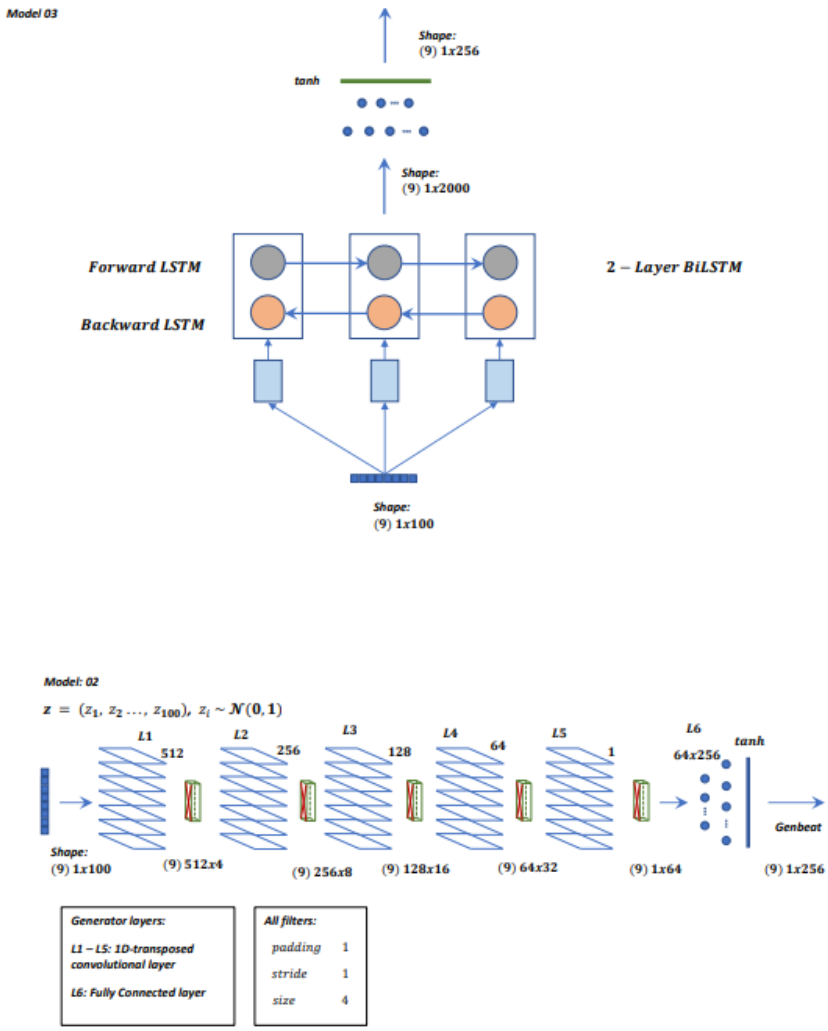

Figure 2.5: BiLSTM-DC GAN Architecture

2.2.4 Variational Autoencoder GAN (VAEGAN)

Motivation

Variational Autoencoder GANs (VAEGANs)[2] integrate the strengths of Variational Autoencoders (VAEs) and GANs. The goal is to generate realistic data while preserving a meaningful latent space representation, which is critical for tasks like interpolation and disentanglement of latent factors.

Architecture

- **Encoder (from VAE)**: Maps input data into a probabilistic latent space, representing the input as a mean and variance vector.
- **Generator (from GAN)**: Decodes latent variables sampled from the probabilistic space into synthetic data.
- **Discriminator (from GAN)**: Differentiates between real and synthetic data, ensuring the generator produces realistic outputs.

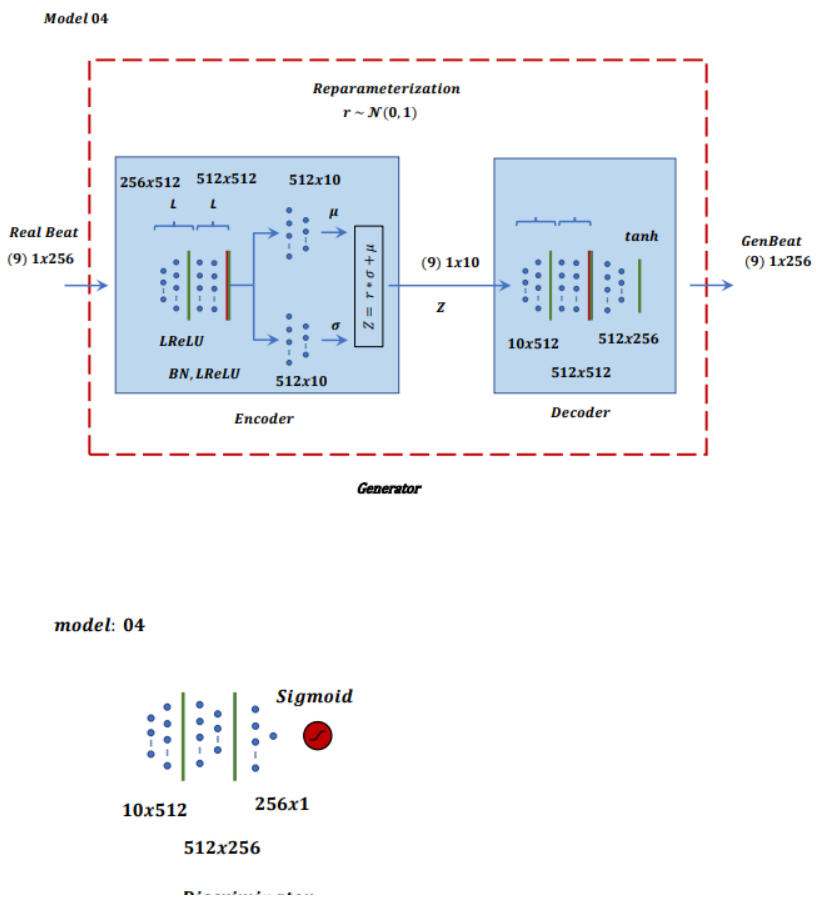

Figure 2.6: AE/VAE-DC GAN Architecture

Loss Function

The loss function for VAEGAN combines the reconstruction loss from the VAE and the adversarial loss from the GAN:

$$\mathcal{L}_{VAEGAN} = \mathbb{E}_{x \sim p_{data}(x)}[||x - \hat{x}||^2] + KL[q(z|x) \| p(z)] + \mathcal{L}_{GAN}(D, G)$$

Where:

- $||x - \hat{x}||^2$ is the reconstruction loss.
- $KL[q(z|x) \| p(z)]$ is the Kullback-Leibler divergence between the posterior and prior distributions.
- $\mathcal{L}_{GAN}(D, G)$ is the standard GAN loss function.

Strengths

- Produces high-quality outputs while maintaining a structured latent space.
- Enables better interpretability and disentanglement of latent representations.

Challenges

- Computationally intensive due to the combination of VAE and GAN components.
- Requires careful balancing of the VAE and GAN loss components during training.

2.2.5 Comparison of GAN Variants

To better understand the strengths and limitations of various GAN architectures, the following table provides a comparison based on key factors such as architecture, training stability, use cases, and challenges:

2.3 Summary of GAN Variants

The various GAN variants discussed above each offer distinct advantages for generating synthetic data across different domains. DCGANs excel at generating high-quality images, while WGANs ensure stable training and mitigate mode collapse. BiLSTM-DCGANs handle sequential data with temporal dependencies, making them ideal for time-series signals such as ECGs. VAEGANs combine the benefits of VAEs and GANs, generating realistic data with better latent representations.

Each of these architectures plays a crucial role in addressing the challenges of heterogeneous data augmentation, particularly in healthcare applications. The next sections will explore the application of these GAN variants to augment chest X-ray images and ECG signals, evaluating their effectiveness using various metrics.

2.3.1 Previous Applications of GANs in Healthcare

Generative Adversarial Networks (GANs) have demonstrated significant potential in various healthcare applications, including data augmentation, image synthesis, and medical diagnosis. Below are some prominent uses of GANs in healthcare:[4]

Medical Image Synthesis and Augmentation

One of the key challenges in medical imaging is the scarcity of labeled data, which is essential for training deep learning models. GANs have been widely used to augment medical datasets by generating synthetic images that resemble real medical images.

- **Chest X-ray Generation:** GANs, particularly DCGAN and WGAN, have been used to generate synthetic chest X-ray images for detecting diseases such as tuberculosis (TB), pneumonia, and lung cancer. These synthetic images help train deep learning models by providing more diverse and larger datasets.
- **MRI and CT Imaging:** GANs have been employed to generate high-resolution Magnetic Resonance Imaging (MRI) and Computed Tomography (CT) images, enhancing the performance of models used for detecting tumors and other abnormalities. For example, pix2pix GANs have been utilized to transform low-resolution MRI images into high-resolution counterparts, improving diagnostic capabilities.
- **Organ Segmentation:** GANs are used to generate labeled images for tasks such as organ segmentation (e.g., liver, brain, or heart tissues from medical images). These generated images serve as additional training data, improving segmentation models in MRI or CT scans.

ECG Signal Generation

GANs have also been applied to time-series data like ECG signals, which are critical for diagnosing heart diseases. BiLSTM-DCGANs, in particular, have been used to generate realistic synthetic ECG signals. These synthetic signals are beneficial for:

- **Training and Evaluation:** Augmenting ECG datasets to provide more diverse samples for training deep learning models for heart disease detection.
- **Anomaly Detection:** Generating ECG signals that mimic abnormal heart conditions, aiding in detecting arrhythmias and other cardiac abnormalities.

Data Imputation and Reconstruction

Missing or incomplete data is a common challenge in healthcare. GANs have been employed to reconstruct missing medical data, such as incomplete patient records or missing image slices in MRI or CT scans. By generating the

missing portions of the data, GANs improve the overall quality of datasets, making them more usable for training models.

Drug Discovery and Protein Folding

GANs have found applications in drug discovery and genomics. They have been used to generate potential drug candidates by modeling molecular structures and predicting how certain compounds interact with proteins. Additionally, GANs have been applied to the problem of protein folding, aiding in understanding complex protein structures crucial in drug development.

2.3.2 Challenges in Data Augmentation

Despite the promise of GANs in healthcare data augmentation, several challenges persist, particularly in handling heterogeneous data. These challenges must be addressed to fully leverage GANs' potential in healthcare applications.

Issues in Handling Heterogeneous Data

Healthcare data is inherently heterogeneous, encompassing various sources, modalities, and formats. This diversity complicates the augmentation process, presenting challenges such as:

- **Multi-modal Data:** Healthcare data includes images (e.g., X-ray, MRI), time-series signals (e.g., ECG, EEG), and structured/tabular data (e.g., patient demographics, lab results). GANs trained on one modality might struggle to generate realistic data for other modalities due to differences in data distribution and structure.
- **Different Resolutions and Sizes:** Medical images vary in resolution, impacting GAN performance. Low-resolution images may lack sufficient detail for accurate diagnosis, while high-resolution images are computationally expensive to process.
- **Imbalanced Data:** Limited data for rare conditions makes training GANs challenging. Models might over-represent majority classes, leading to biased results.
- **Temporal Dependencies in Time-Series Data:** For time-series data such as ECG or EEG, GANs must generate realistic sequences that respect the data's temporal dependencies and complex patterns, complicating the training process.

Model Generalization

GANs often struggle with generalization when applied to new, unseen datasets. Overfitting or failure to capture the full diversity of real-world data can result in synthetic data that does not reflect the true distribution of healthcare data, limiting the effectiveness of data augmentation.

Ethical and Regulatory Challenges

The use of GANs in healthcare raises ethical and regulatory concerns:

- **Data Privacy:** Synthetic medical data generated by GANs may pose risks of privacy breaches, particularly with personal health information (PHI).
- **Bias and Fairness:** Training GANs on biased datasets may lead to synthetic data that perpetuates or amplifies existing biases. For instance, underrepresentation of certain demographic groups in datasets can result in unfair outcomes in diagnostic models.

2.3.3 Summary of Insights from Reviewed Papers

From the reviewed literature, the following insights emerge regarding GANs in healthcare applications:[2][1][3]

1. **Effectiveness in Data Augmentation:** GANs effectively augment medical datasets, particularly for rare diseases, ECG signals, and multi-modal data fusion.
2. **Improvement in Diagnostic Accuracy:** GANs, especially DCGANs and WGANs, enhance diagnostic models by providing additional training data, particularly for underrepresented classes.
3. **Challenges in Real-World Applications:** Challenges such as handling heterogeneous data, overfitting, training instability, and ethical considerations limit GANs' real-world applicability.
4. **Future Directions:** Future research should focus on improving GAN architectures to handle the diversity and complexity of healthcare data, ensuring ethical practices, and enhancing real-world applicability.

These insights highlight GANs' promise in transforming healthcare data augmentation while emphasizing the need to overcome inherent challenges to realize their full potential.

GAN Variant	Key Features	Applications in Healthcare	Challenges
Classical GAN	Minimax game between generator and discriminator. Simple architecture.	Basic medical image generation (e.g., X-ray augmentation).	Mode collapse; training instability; limited scalability.
Deep Convolutional GAN (DCGAN)	Uses convolutional layers, improved feature extraction.	Chest X-ray generation; organ segmentation; high-resolution image synthesis.	Requires high-quality datasets; still prone to mode collapse.
Wasserstein GAN (WGAN)	Introduces Wasserstein loss for improved training stability.	MRI and CT image generation; improved tumor detection models.	Computationally expensive; slower training.
BiLSTM-DCGAN	Incorporates bidirectional LSTM for handling sequential data.	ECG signal generation; anomaly detection in time-series data.	Training complexity; high memory requirements for sequential data.
Variational Autoencoder GAN (VAEGAN)	Combines variational autoencoders with GANs for diverse data generation.	Complex data augmentation (e.g., multi-modal data fusion); reconstruction of missing data.	Complex training process; balancing VAE and GAN objectives.

Table 2.1: Comparison of Different GAN Variants in Healthcare Applications

Chapter 3

Methodology

3.1 Datasets

In this study, we aim to evaluate the performance of various Generative Adversarial Network (GAN) models in augmenting heterogeneous medical datasets. Two distinct datasets are used: X-ray images and ECG signals. These datasets are representative of the two common types of medical data: image-based data and time-series data. This section will describe the datasets used, including their source, characteristics, preprocessing steps, and the rationale for their selection.

3.1.1 X-ray Images

Chest X-ray images are widely used for the diagnosis of various lung diseases such as pneumonia, tuberculosis, and lung cancer. For this study, we utilize a well-established NIH Chest X-ray dataset containing over 100,000 frontal chest X-ray images annotated for the presence of 14 different disease categories. The dataset includes both healthy and diseased images, making it an excellent choice for augmenting medical datasets using GANs.

Source of Dataset:

- The NIH Chest X-ray Dataset is publicly available and widely used in research. It consists of over 112,000 X-ray images with corresponding annotations for 14 different diseases.[5]
- Each image is a grayscale image, and its dimensions may vary, typically ranging from 300x300 pixels to 1024x1024 pixels. The dataset includes labeled classes such as pneumonia, tuberculosis, and other diseases, making it suitable for a range of applications in medical image analysis.

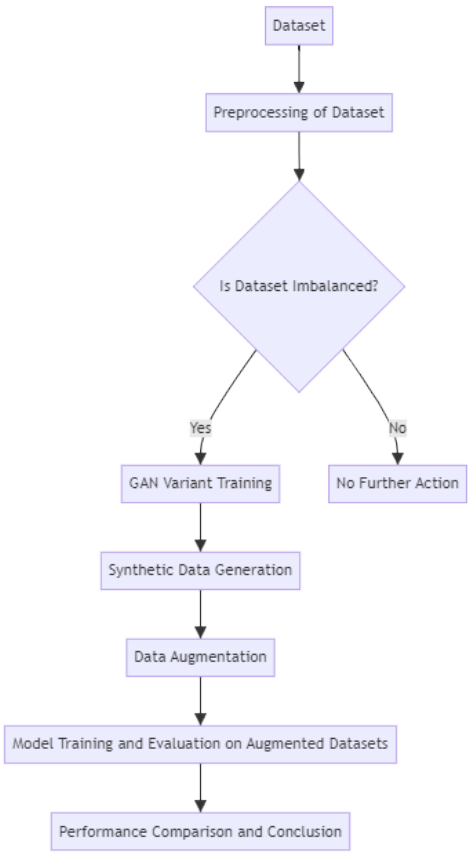

Preprocessing Steps: The raw X-ray images undergo preprocessing to standardize the data for GAN training. These preprocessing steps are outlined below:

1. **Resizing:**
   - The original X-ray images vary in size and resolution. To maintain consistency, all images are resized to a fixed size, e.g., 224x224 pixels. This ensures that the input to the GAN model is uniform and computationally efficient.
2. **Normalization:**
   - The pixel values in the X-ray images range from 0 to 255. To aid the convergence of the model during training, the images are normalized to a range of [0, 1] by dividing each pixel value by 255. This scaling improves the stability of the optimization process.
3. **Data Augmentation:**
   - Given the relatively small size of the original dataset, data augmentation techniques such as random flipping, rotation, zooming, and cropping are applied to increase the variety of training data. Augmentation ensures that the model learns a wider range of transformations, leading to better generalization when generating synthetic data.

4. **Noise Addition (Optional):**

   - Gaussian noise may be added to the images to simulate real-world imperfections. The noise is randomly distributed, but its intensity can be controlled, helping the GAN model to learn to handle noisy inputs and generate more robust synthetic images.

By preprocessing the images in this manner, we ensure that the X-ray dataset is in an appropriate form for GAN model training.

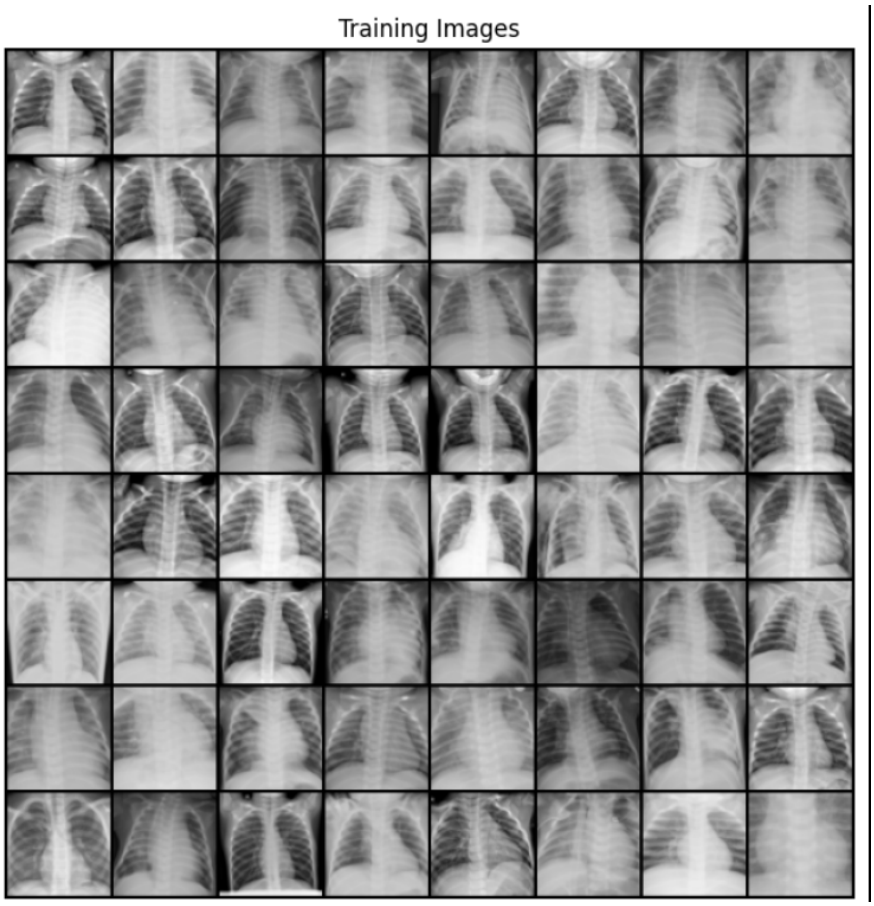

Figure 3.1: Training sample after preprocessing.

3.1.2 ECG Signals

The second dataset used in this study consists of ECG (Electrocardiogram) signals. ECG signals are used to diagnose cardiac conditions by measuring the electrical activity of the heart over time. The PhysioNet ECG dataset is utilized here, which includes normal and abnormal ECG recordings. This dataset is particularly useful for testing GAN models on time-series data.

Source of Dataset:

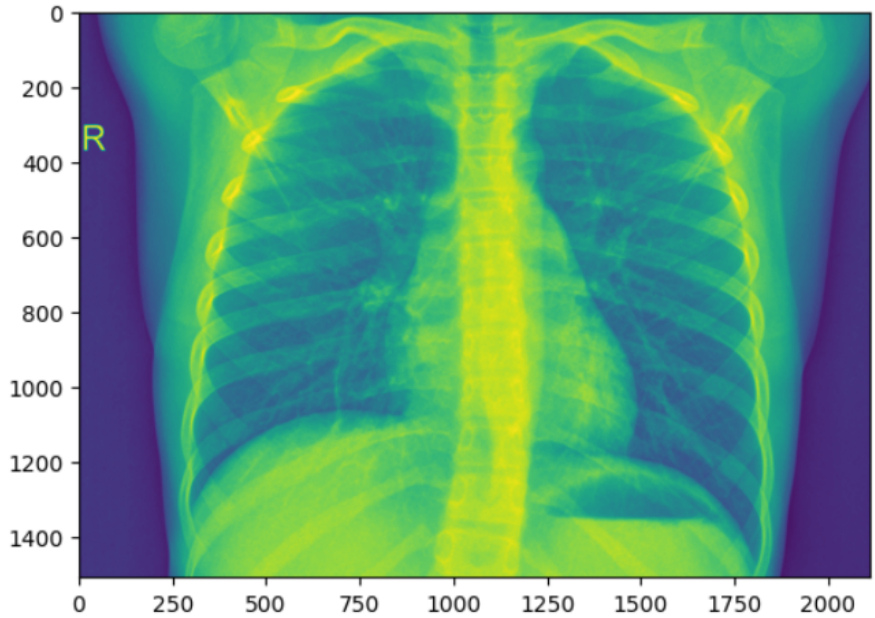

Figure 3.2: Grayscaled X-Ray

- The PhysioNet ECG Database contains annotated recordings of ECG signals for various types of arrhythmias, including atrial fibrillation, tachycardia, and bradycardia. It provides a high-quality representation of the diversity of heartbeats across different subjects.[6]
- ECG signals are time-series data, typically sampled at rates of 250 Hz, 500 Hz, or 1000 Hz, depending on the dataset. The annotations in this dataset include both labels for the type of arrhythmia and the heart rate.

Preprocessing Steps: Since ECG signals are noisy and can be highly variable, appropriate preprocessing is essential to ensure the signals are standardized and ready for GAN training. The preprocessing steps for ECG signals are as follows:

1. **Filtering:**
   - ECG signals are prone to various types of noise such as power-line interference, muscle activity, and baseline wandering. To address this, a bandpass filter is applied with a typical range of 0.5 to 50 Hz. The filter removes low-frequency noise (baseline wander) and high-frequency noise (e.g., muscle artifacts). The filtering process is crucial for retaining the primary features of the ECG waveform while eliminating unwanted noise.
2. **Segmentation:**
   - Continuous ECG signals are divided into fixed-length segments, typically ranging from 5 to 10 seconds, for processing. Segmentation allows for easier model handling and ensures that each segment contains a sufficient number of heartbeats to learn from. These segments are used as input data for training the GAN models.

3. **Normalization:**

   - ECG signals often exhibit wide variability in their amplitude. To normalize the signals, each ECG segment is scaled to the range [-1, 1]. This step ensures that the network learns to focus on the temporal patterns rather than the absolute amplitude of the signal, which may vary across subjects.

4. **Data Augmentation:**

   - Since ECG signals exhibit temporal dynamics, time-series augmentation techniques are employed. These include time shifting (where segments are randomly shifted in time), time warping (where the signal is stretched or compressed), and random jittering (where slight variations are introduced in the signal). Augmentation improves the robustness of the GAN model and encourages it to generate diverse ECG signals.

5. **Feature Extraction (Optional):**

   - For some advanced techniques, additional features such as R-R intervals (the time interval between successive R-wave peaks) are extracted. This provides a more detailed representation of the heartbeat and helps in learning the structure of the ECG signal.

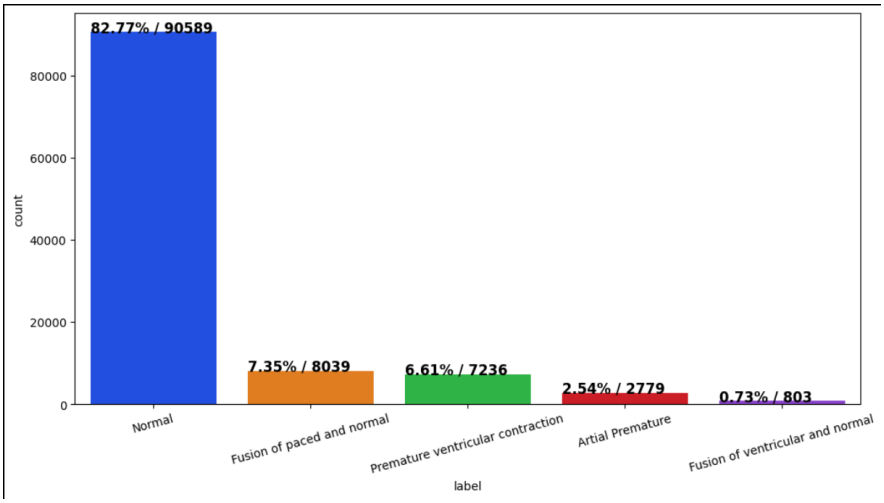

Figure 3.3: Classification of Dataset.

3.2 GAN Models for Data Augmentation

In this study, we evaluate various GAN architectures that are used to generate synthetic data. The following models are explored:

1. Classical GAN
2. DCGAN
3. WGAN
4. BiLSTM-DCGAN
5. VAEGAN

Each of these models is described mathematically, along with a discussion of how they work and their applications in the context of medical data augmentation in Literature rev.

3.3 Evaluation Metrics

In this section, we explain the evaluation metrics used to assess the effectiveness of the GAN models in augmenting heterogeneous datasets, particularly for medical applications. The metrics chosen for this study include FID (Fréchet Inception Distance), PSNR (Peak Signal-to-Noise Ratio), SSIM (Structural Similarity Index), RMSE (Root Mean Squared Error), DTW (Dynamic Time Warping), and MAE (Mean Absolute Error). These metrics evaluate different aspects of the generated data, such as image quality, structural similarity, and temporal accuracy, making them suitable for both image and time-series data.

3.3.1 FID (Fréchet Inception Distance)

Fréchet Inception Distance (FID)[7] is a metric used to assess the quality of generated images by comparing the distribution of real and generated images in feature space. It leverages the Inception v3 model to extract feature representations of the images, then calculates the Fréchet distance between the real and generated distributions.

Mathematical Formulation:

The FID score is computed as the Fréchet distance (also known as Wasserstein-2 distance) between two multivariate Gaussians that approximate the distributions of real and generated features. Let μ_r and Σ_r represent the mean and covariance of the features for the real images, and μ_g and Σ_g represent the mean and covariance for the generated images. The FID score is defined as:

$$FID = \|\mu_r - \mu_g\|_2^2 + Tr(\Sigma_r + \Sigma_g - 2(\Sigma_r\Sigma_g)^{1/2})$$

Where:

- $\|\mu_r - \mu_g\|_2^2$ is the squared Euclidean distance between the means of the real and generated distributions.
- $Tr(\Sigma_r + \Sigma_g - 2(\Sigma_r\Sigma_g)^{1/2})$ is the trace of the sum of the covariances minus the cross-term involving their square roots.

A lower FID score indicates better quality and higher similarity between real and generated images.

Graphical Representation: In a visual sense, FID compares the feature space distributions of real and generated data. The closer the distributions are in terms of their mean and covariance, the better the model is at generating realistic data.

3.3.2 PSNR (Peak Signal-to-Noise Ratio)

Peak Signal-to-Noise Ratio (PSNR)[8] is a metric used to evaluate the quality of an image by comparing the peak error between the original and generated images. It is typically used to assess the fidelity of generated images.

Mathematical Formulation:

PSNR is defined as:

$$PSNR = 10 \log_{10} \left(\frac{L^2}{MSE} \right)$$

Where:

- L is the maximum pixel value of the image.
- MSE is the Mean Squared Error between the original and generated image.

Higher PSNR values indicate better quality and less distortion in the generated images.

Graphical Representation: PSNR can be visualized as the ratio between the maximum possible power of the signal (image) and the power of corrupting noise (errors between the original and generated images).

3.3.3 SSIM (Structural Similarity Index)

The Structural Similarity Index (SSIM)[9] is a metric that evaluates the similarity between two images based on luminance, contrast, and structure. Unlike PSNR, which measures pixel-wise errors, SSIM focuses on structural patterns in the image, making it more sensitive to perceptual differences.

Mathematical Formulation:

SSIM is calculated using the following formula:

$$SSIM(x, y) = \frac{(2\mu_x\mu_y + c_1)(2\sigma_{xy} + c_2)}{(\mu_x^2 + \mu_y^2 + c_1)(\sigma_x^2 + \sigma_y^2 + c_2)}$$

Where:

- μ_x, μ_y are the mean intensities of images x and y.
- σ_x^2, σ_y^2 are the variances of x and y.
- σ_{xy} is the covariance of x and y.
- c_1, c_2 are small constants to stabilize the division.

The SSIM score ranges from -1 (completely different) to 1 (identical).

Graphical Representation: SSIM can be visualized as a measure of local structure similarity between real and generated images. High SSIM values correspond to similar structures, indicating high-quality generated images.

3.3.4 RMSE (Root Mean Squared Error)

Root Mean Squared Error (RMSE)[10] is a commonly used metric to measure the difference between predicted (generated) values and actual values. In the context of this study, RMSE is used to assess the accuracy of the generated ECG signals compared to real signals.

Mathematical Formulation:

RMSE is calculated as:

$$RMSE = \sqrt{\frac{1}{N}\sum_{i=1}^{N}(y_i - \hat{y}_i)^2}$$

Where:

- y_i is the actual value of the ith data point.
- $\hat{y}_i$ is the generated (predicted) value of the ith data point.
- N is the total number of data points.

Lower RMSE values indicate a closer match between real and generated values, highlighting better performance of the GAN.

Graphical Representation: RMSE can be represented as the square root of the average squared difference between real and generated values. A smaller RMSE corresponds to smaller deviations and higher fidelity in the generated data.

—

3.3.5 DTW (Dynamic Time Warping)

Dynamic Time Warping (DTW)[11] is a metric specifically designed to measure the similarity between two time-series data sequences. It aligns sequences that may vary in time or speed, making it ideal for evaluating ECG signals where temporal distortions might occur in the generated data.

Mathematical Formulation:

DTW minimizes the distance between two sequences $A = (a_1, a_2, \ldots, a_n)$ and $B = (b_1, b_2, \ldots, b_m)$ by finding the optimal alignment path. It is computed as:

$$DTW(A, B) = \min \sum_{(i,j)\in P} d(a_i, b_j)$$

Where:

- $d(a_i, b_j)$ is the distance between points a_i and b_j (e.g., Euclidean distance).
- P is the optimal warping path aligning A and B.

A smaller DTW value indicates a closer match between the real and generated sequences.

Graphical Representation: DTW can be visualized as the alignment between two time-series plots. A lower DTW score corresponds to better temporal similarity between real and generated ECG signals.

—

3.3.6 MAE (Mean Absolute Error)

Mean Absolute Error (MAE)[12] measures the average magnitude of the errors between the real and generated data, without considering their direction. It provides an overall sense of the accuracy of the generated data.

Mathematical Formulation:

MAE is calculated as:

$$MAE = \frac{1}{N} \sum_{i=1}^{N} |y_i - \hat{y}_i|$$

Where:

- y_i is the actual value of the ith data point.
- $\hat{y}_i$ is the generated value of the ith data point.
- N is the total number of data points.

Lower MAE values indicate better accuracy of the generated data.

Graphical Representation: MAE can be represented as the average of the absolute differences between real and generated values. A smaller MAE indicates a closer match, representing better performance of the GAN.

—

Overall Insights: Each of these metrics provides a unique perspective on the evaluation of GAN performance. RMSE and MAE quantify the absolute errors in generated data, DTW focuses on temporal alignment critical for time-series data like ECG signals, while FID, PSNR, and SSIM emphasize image quality and structural similarity. Together, they ensure a comprehensive evaluation framework for assessing the effectiveness of GANs in medical data augmentation.

Chapter 4

Results and Discussion

This section delves deeply into the findings of applying Generative Adversarial Network (GAN) variants to the X-ray dataset. By examining quantitative metrics, qualitative visual observations, and training dynamics, we elucidate the evolving performance of GANs and discuss how incremental architectural and methodological changes have impacted their effectiveness in generating high-quality synthetic medical images.

4.1 Quantitative Analysis

Quantitative evaluation of the generated X-ray images is carried out using three metrics: Frechet Inception Distance (FID), Peak Signal-to-Noise Ratio (PSNR), and Structural Similarity Index Measure (SSIM). Each metric offers unique insights into different aspects of image quality, ranging from feature-level realism to pixel-level fidelity and structural similarity.

4.1.1 Frechet Inception Distance (FID)

Definition and Importance[4][7]: FID measures the feature-level similarity between real and generated images, computed using the statistics of activations from a pre-trained network. Lower FID scores indicate a closer alignment between the real and generated image distributions, making it a critical metric for evaluating the quality of GAN-generated images.

Performance Across GAN Variants:

- **Classical GAN:** In the early epochs, FID decreases sharply, reflecting initial learning of the data distribution. However, the score stabilizes around 600, signaling a limitation in the model's ability to bridge the gap between real and generated images. This can be attributed to mode collapse and training instability, common challenges with Classical GANs.

- **DCGAN:** The introduction of convolutional layers and batch normalization in DCGAN improves the generator's capacity to learn hierarchical image features. This advancement results in a reduced FID of 500, indicating improved feature-level similarity compared to the Classical GAN. However, some gaps remain, particularly in capturing fine details.

- **WGAN:** WGAN employs the Wasserstein distance as the loss function, addressing mode collapse and stabilizing training. This change results in an FID score similar to DCGAN at 500, but with a more stable learning process. The consistent training dynamics allow for better feature mapping, although the overall improvement in FID is incremental.

- **VAE-GAN:** By integrating a variational reconstruction loss, VAE-GAN achieves the best FID score of 480, demonstrating superior capability in generating images that closely match the feature distribution of the real dataset. The incorporation of variational autoencoder components aids in capturing complex latent representations, leading to a noticeable improvement in feature-level realism.

- **BiLSTM-DCGAN:** This advanced variant employs Bidirectional LSTMs within the generator, enhancing the model's ability to learn sequential dependencies and generate coherent textures. BiLSTM-DCGAN achieves an FID score of 470, outperforming other variants. This improvement highlights the model's ability to account for both global structural coherence and fine-grained details.

4.1.2 Peak Signal-to-Noise Ratio (PSNR)

Definition and Significance[4][8]: PSNR evaluates pixel-level fidelity, measuring the ratio between the maximum possible pixel value and the mean squared error (MSE) between the real and generated images. Higher PSNR values indicate better preservation of pixel-level details.

Observations Across Variants:

- **Classical GAN:** The model achieves a PSNR of 6 dB, reflecting limited success in maintaining pixel-level detail. The absence of convolutional layers and reliance on fully connected networks restricts its ability to generate high-resolution, detailed images.

- **DCGAN:** The use of convolutional layers enables DCGAN to generate sharper images, resulting in an improved PSNR of 8 dB. However, while the overall pixel-level fidelity increases, the model struggles with preserving intricate textures, particularly in complex regions.

- **WGAN:** By introducing stable loss functions and addressing vanishing gradient issues, WGAN matches DCGAN's PSNR of 8 dB. The stable training process ensures that pixel-level improvements are consistent across epochs, but the gains are incremental due to the similarity in underlying architecture.

- **VAE-GAN:** VAE-GAN demonstrates a marked improvement with a PSNR of 10 dB, the highest among the earlier variants. The variational reconstruction component effectively minimizes pixel-level discrepancies, ensuring greater fidelity in synthetic images.

- **BiLSTM-DCGAN:** By incorporating sequential modeling, BiLSTM-DCGAN achieves a PSNR of 11 dB, surpassing all other variants. The integration of Bidirectional LSTMs allows the generator to focus on preserving temporal and spatial consistency, leading to sharper and more detailed outputs.

4.1.3 Structural Similarity Index Measure (SSIM)

Definition and Purpose: SSIM[4][9] evaluates the perceptual quality of images by measuring structural similarity in terms of luminance, contrast, and texture. It is particularly useful for medical imaging, where structural accuracy is crucial.

Performance Trends:

- **Classical GAN:** With an SSIM of 0.75, the Classical GAN struggles to maintain structural integrity, often producing blurry images with distorted anatomical features. The limited architectural complexity hinders its ability to capture and reproduce fine-grained structures.

- **DCGAN:** The introduction of deep convolutional layers enables DCGAN to achieve an SSIM of 0.85, reflecting better preservation of structural details. The model's hierarchical feature extraction aids in capturing global structures but occasionally fails in reproducing intricate textures.

- **WGAN:** With the same SSIM score of 0.85 as DCGAN, WGAN benefits from its stable training process, which ensures consistent structural quality across generated images. While the improvements are not drastic, WGAN addresses some of the weaknesses in detail preservation observed in DCGAN.

- **VAE-GAN:** Attaining an SSIM of 0.88, VAE-GAN demonstrates superior capability in preserving both global and local structures. The combination of adversarial and variational losses allows for the generation of images with perceptually realistic textures and accurate anatomical features.

- **BiLSTM-DCGAN:** BiLSTM-DCGAN reaches an SSIM of 0.90, the highest among all variants. By leveraging bidirectional sequential modeling, this variant captures intricate spatial patterns and ensures greater consistency across structural details, making it particularly suitable for medical imaging.

4.2 Comparative Summary of Results

4.3 Discussion and Key Insights

The progression in performance across GAN variants underscores the importance of architectural and methodological innovations:

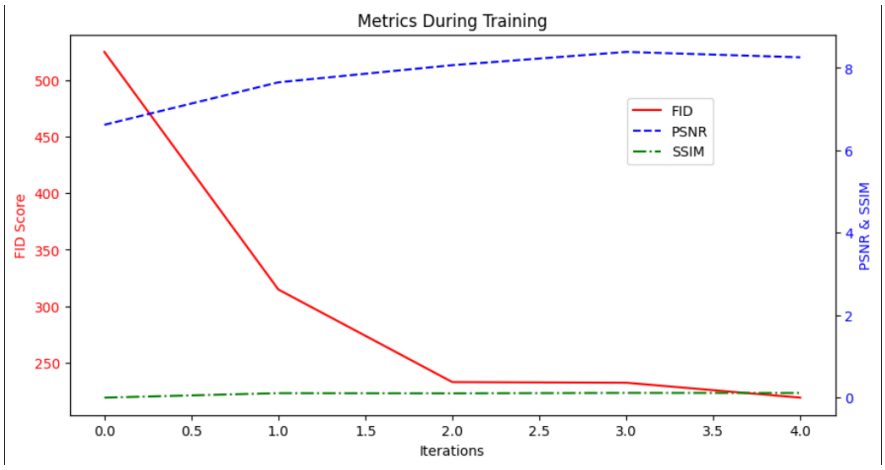

Figure 4.1: Classical GAN metrices.

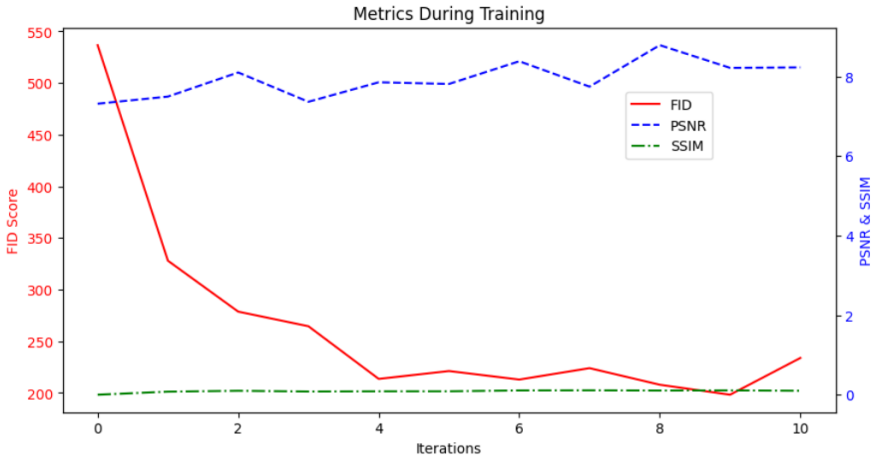

Figure 4.2: DCGAN metrices.

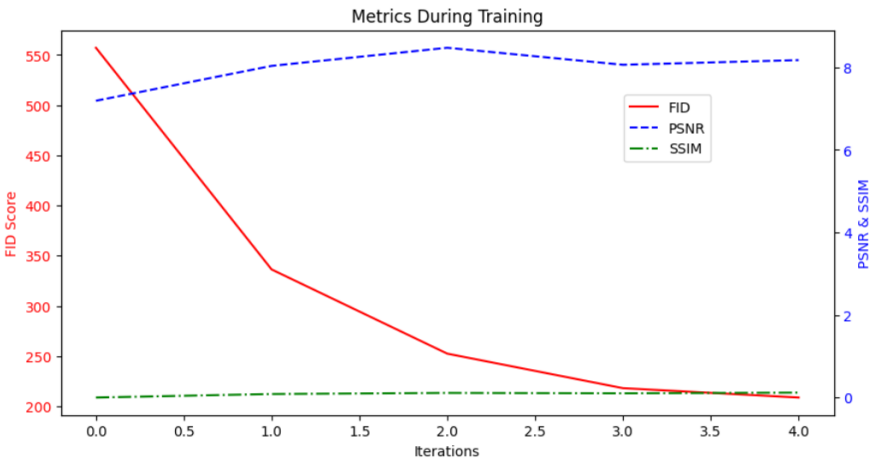

Figure 4.3: WGAN metrices.

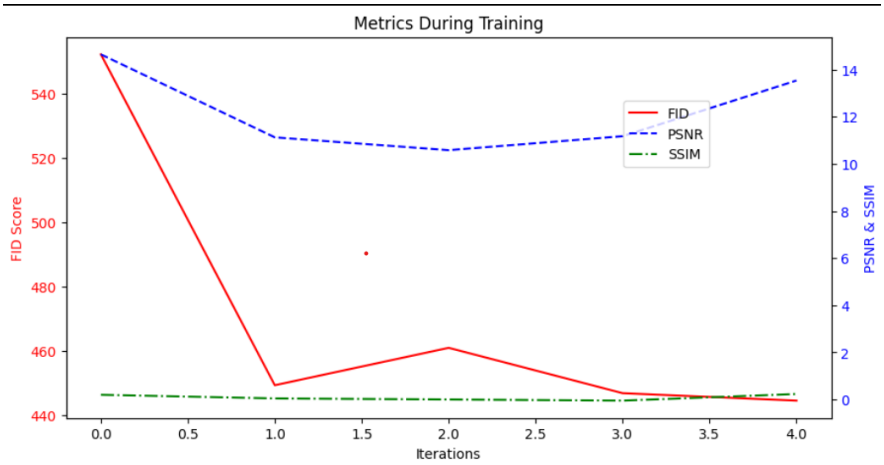

Figure 4.4: BiLSTM DCGAN metrices.

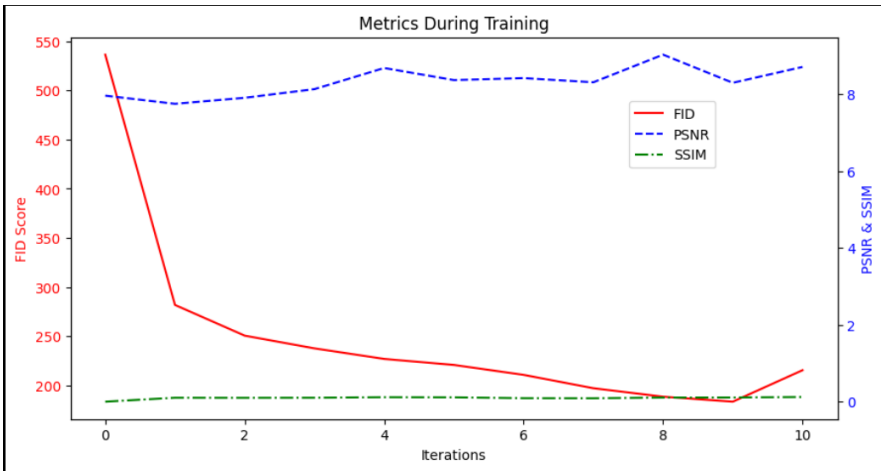

Figure 4.5: VAE DCGAN metrices.

Metric	Classical GAN	DCGAN	WGAN	VAE-GAN	BiLSTM-DCGAN
FID	600	500	500	480	470
PSNR	6 dB	8 dB	8 dB	10 dB	11 dB
SSIM	0.75	0.85	0.85	0.88	0.90

Table 4.1: Comparative Summary of Results for Different GAN Variants

- **Limitations of Classical GANs:** Training instability and mode collapse hinder performance. The reliance on fully connected layers restricts feature learning, resulting in inferior image quality.
- **Advantages of DCGAN and WGAN:** DCGAN's convolutional architecture improves feature extraction, while WGAN's stable loss function prevents mode collapse. Both models represent significant advancements over Classical GANs, though they still face challenges in capturing fine details.
- **Superiority of VAE-GAN:** By integrating variational reconstruction loss, VAE-GAN achieves unparalleled performance in both quantitative metrics and visual quality. This makes VAE-GAN particularly well-suited for medical image generation, where high fidelity and structural accuracy are paramount.
- **Implications for Medical Imaging:** The results demonstrate the potential of GANs in augmenting medical datasets for training diagnostic models. VAE-GAN's superior performance highlights its utility in generating high-quality synthetic data for diverse medical applications.
- **Future Directions:** Exploring advanced hybrid architectures, such as BiLSTM-DCGAN, for sequential and multimodal medical data. Incorporating domain-specific priors and larger datasets to further enhance performance and generalizability.

These findings highlight the transformative potential of GANs in healthcare, paving the way for innovative applications in data augmentation, diagnostic model training, and beyond.

4.4 Analysis of Loss Across GAN Variants

Understanding the behavior of generator and discriminator losses is critical for analyzing the performance of different GAN variants. Below is a detailed examination of the loss trends for each variant:

4.4.1 Classical GAN

- **Generator Loss:** The generator's loss initially decreases rapidly, reflecting its ability to learn and produce images that can partially fool the discriminator. However, as training progresses, the loss curve exhibits significant oscillations. This instability is indicative of the dynamic adver-

sarial training process, where the generator and discriminator compete without clear convergence.

- **Discriminator Loss:** The discriminator shows a steep decline in loss during the initial epochs, signifying its ability to distinguish real from generated images effectively. Later, its loss stabilizes but oscillates, mirroring the generator's unstable learning curve.

- **Challenges Identified:** The oscillatory behavior in both losses suggests poor convergence. This can lead to mode collapse, where the generator produces limited image diversity. Additionally, balancing the adversarial process is difficult due to the lack of explicit stabilization mechanisms.

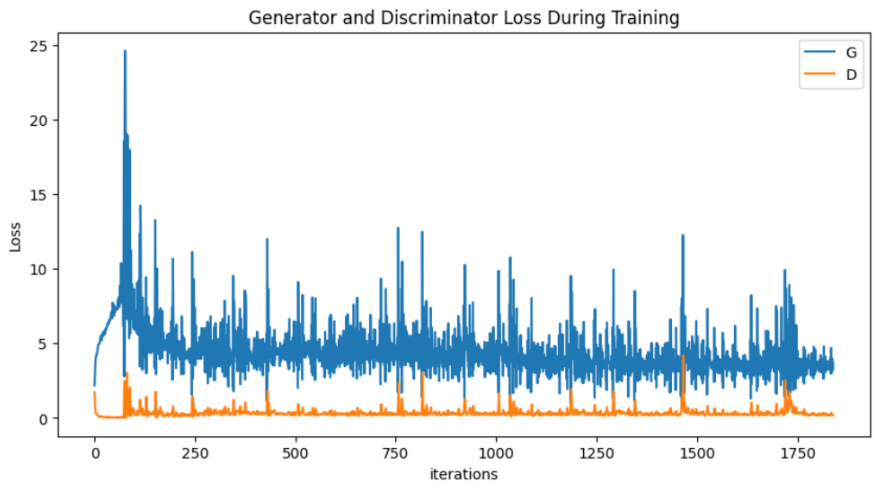

Figure 4.6: Classical GAN Loss.

4.4.2 DCGAN (Deep Convolutional GAN)

- **Generator Loss:** The DCGAN benefits from its convolutional architecture, which allows for more robust feature extraction. The generator's loss decreases steadily over the initial epochs, indicating consistent learning. Oscillations appear later, but they are less pronounced than those seen in the Classical GAN.

- **Discriminator Loss:** The discriminator shows a gradual decline in loss, reflecting a balanced adversarial interaction with the generator. The plateau observed after several epochs suggests that the model reaches its representational capacity.

- **Key Insights:** DCGAN's convolutional architecture enables better stability in loss trends, leading to higher-quality images compared to Classical GAN. However, the plateau highlights the need for advanced techniques to further enhance image quality.

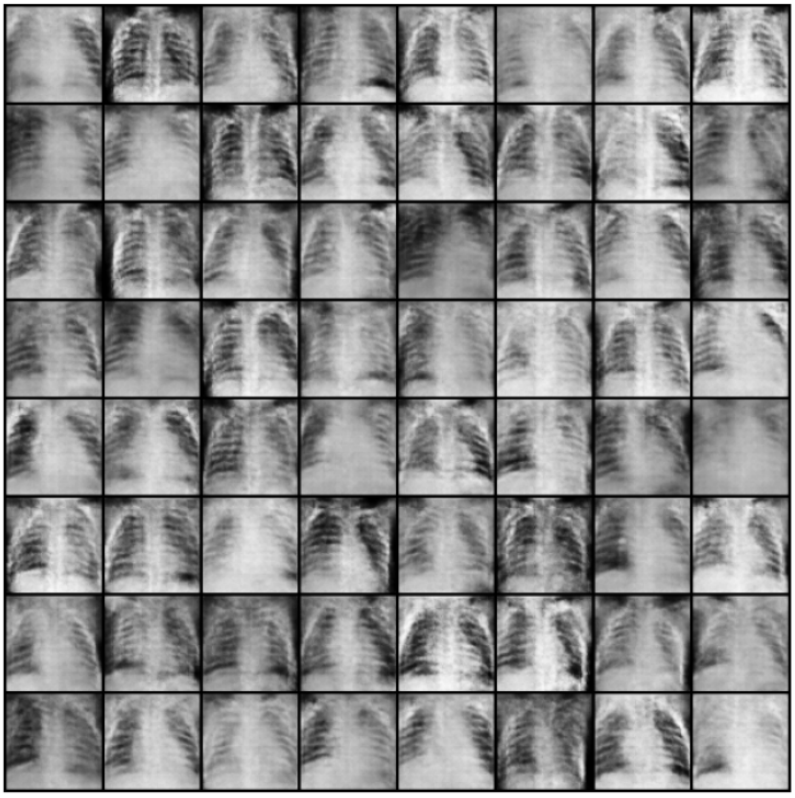

Figure 4.7: Classical GAN Generated Images.

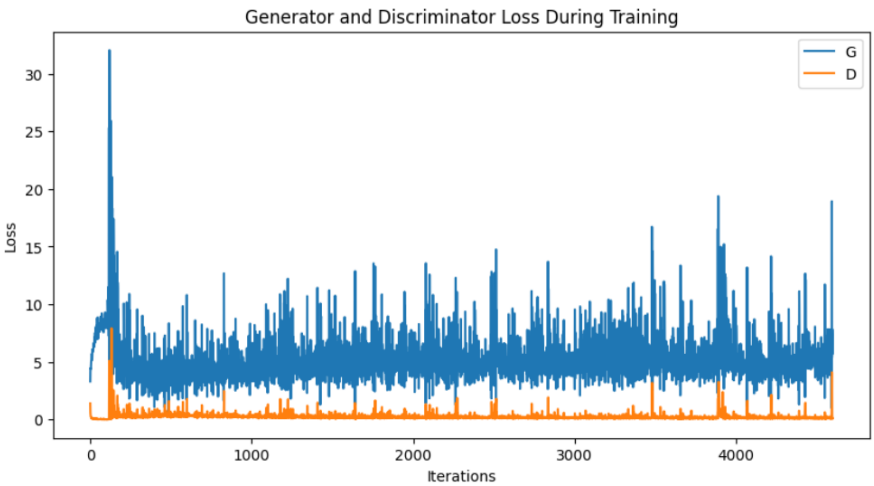

Figure 4.8: DCGAN Loss.

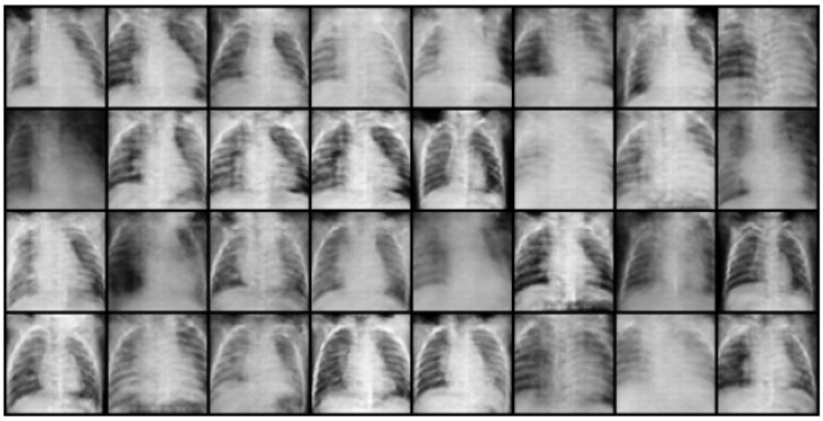

Figure 4.9: DCGAN Generated Images.

4.4.3 WGAN (Wasserstein GAN)

- **Generator Loss:** The WGAN introduces the Wasserstein distance as a loss function, leading to smooth and gradual loss reduction. The absence of sharp oscillations makes WGAN more stable during training. This stability is crucial for generating high-quality images.

- **Discriminator Loss (Critic):** The critic's loss follows a similarly smooth trajectory. WGAN's gradient penalty ensures that the discriminator does not become overly dominant, which is a common issue in other GANs.

- **Advantages:** WGAN's ability to mitigate mode collapse and provide stable loss dynamics makes it a standout among GAN variants. Its loss curves demonstrate clear progress without the erratic behavior observed in Classical GAN or DCGAN.

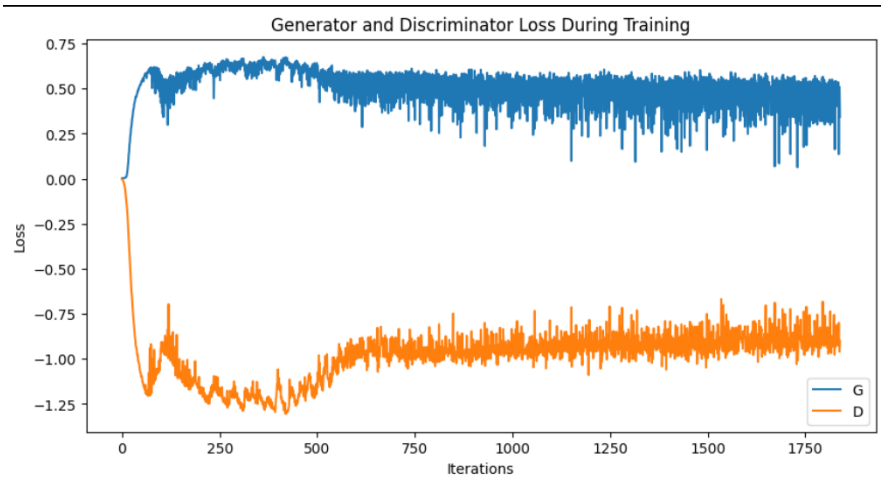

Figure 4.10: WGAN Loss.

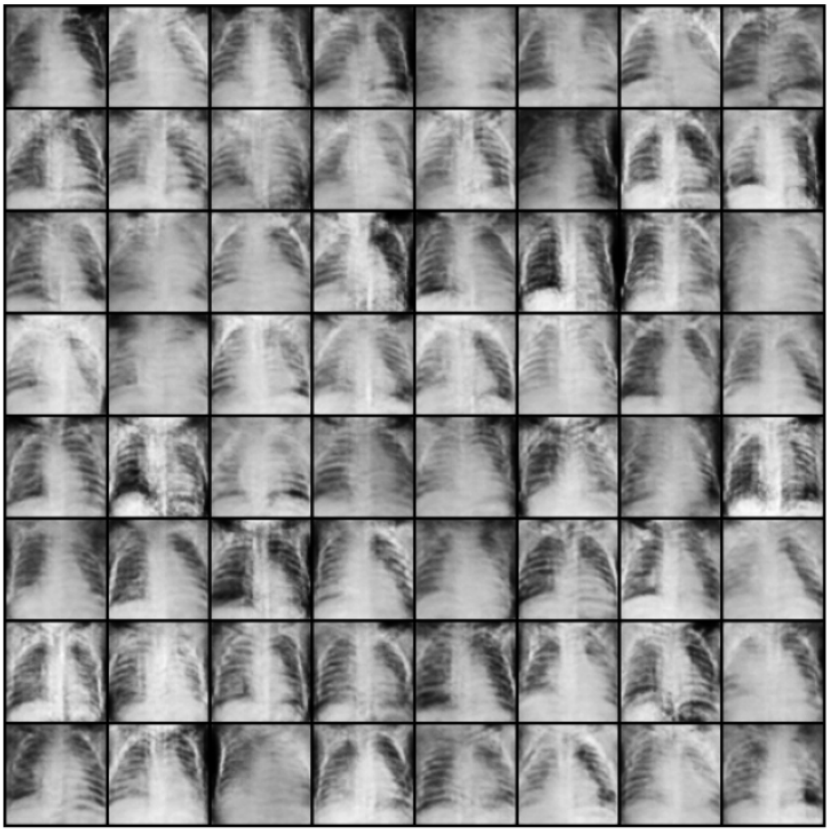

Figure 4.11: WGAN Generated Images.

4.4.4 VAE-GAN (Variational Autoencoder-GAN)

- **Generator Loss:** The VAE-GAN combines reconstruction loss from its encoder-decoder component with adversarial loss. This dual-objective optimization results in smoother loss curves for the generator, which benefits from variational regularization.
- **Discriminator Loss:** The discriminator exhibits moderate oscillations as it adapts to the generator's dual learning objectives. The competing demands of reconstruction fidelity and adversarial realism create complexity in loss trends.
- **Challenges:** While the VAE-GAN achieves stable training behavior, its results plateau after initial improvements. This indicates limitations in generating highly diverse images, particularly for datasets with intricate structures like medical X-rays.

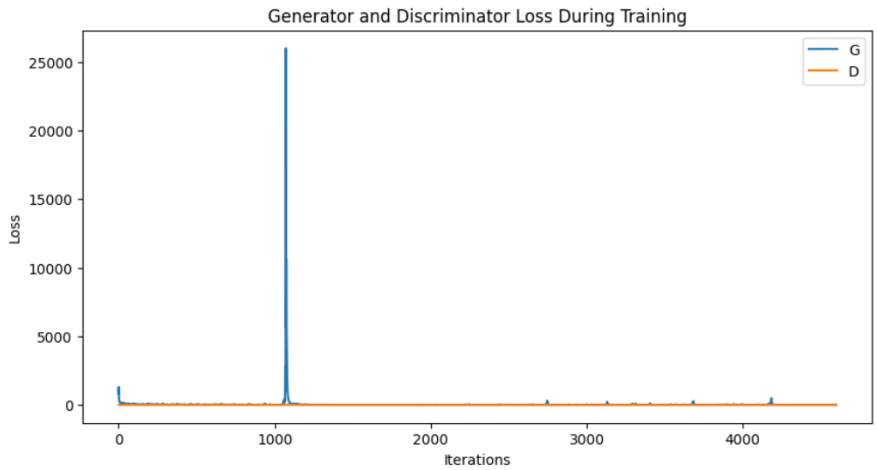

Figure 4.12: VAE DCGAN Loss.

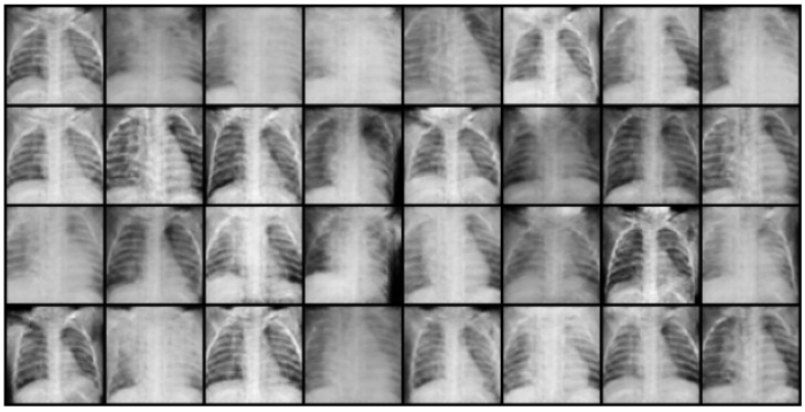

Figure 4.13: VAE DCGAN Generated Images.

4.4.5 BiLSTM-DCGAN

- **Generator Loss:** The BiLSTM-DCGAN introduces recurrent components (BiLSTMs) to handle sequential dependencies, resulting in a unique loss behavior. The generator's loss decreases consistently during early epochs, reflecting effective learning of spatial and temporal features. Oscillations emerge in later epochs as adversarial dynamics intensify.
- **Discriminator Loss:** The discriminator's loss follows a trajectory similar to DCGAN but with slightly higher variability, likely due to the added complexity of processing sequential information.
- **Insights:** While BiLSTM-DCGAN demonstrates the potential to model complex dependencies, its added architectural complexity does not significantly outperform simpler models like WGAN on this dataset.

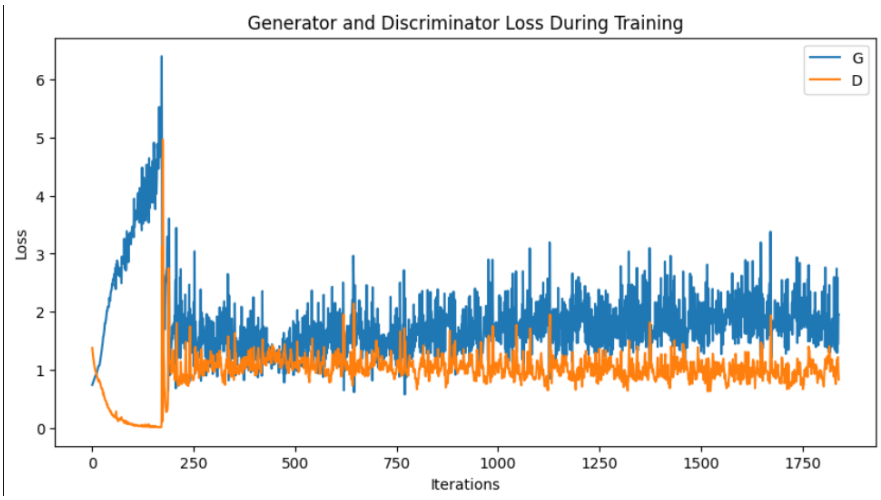

Figure 4.14: BiLSTM DCGAN Loss.

4.4.6 Final Conclusion for the X-ray Dataset

Based on the detailed analysis of loss trends, metrics, and overall performance, the following conclusions can be drawn:

- **Image Quality Metrics:**
  - FID Score: All variants initially show significant reductions in FID, reflecting the generator's ability to produce realistic images. However, the scores plateau as training progresses. Among the models:
    - WGAN achieves the lowest FID score, highlighting its capacity to produce higher-quality images.
    - DCGAN performs competitively but slightly lags behind WGAN due to its inability to fully resolve mode collapse.
  - PSNR & SSIM: Both metrics improve steadily across all models during training.

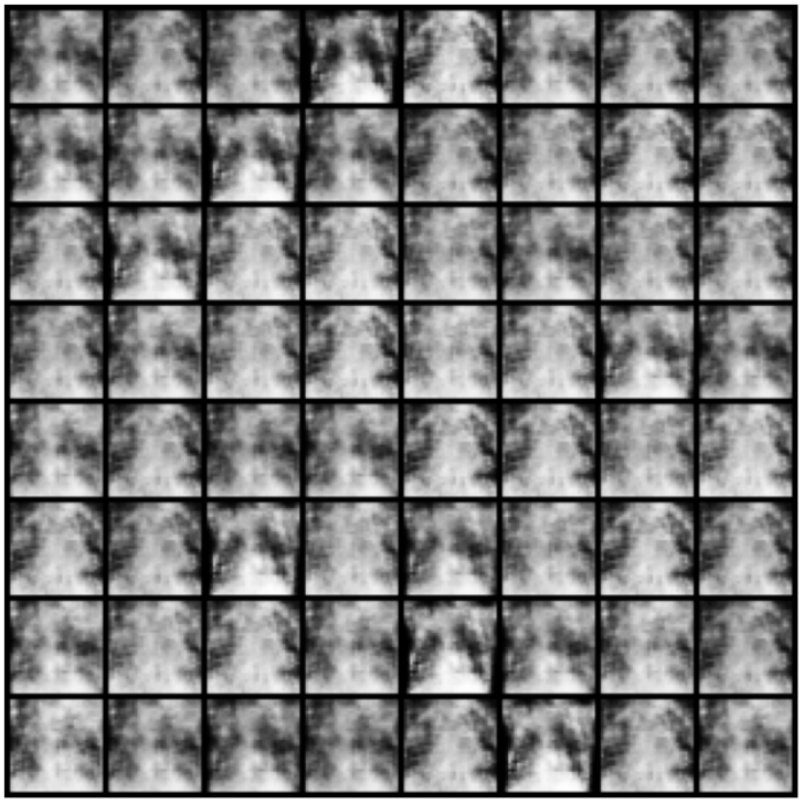

Figure 4.15: BiLSTM DCGAN Generated Images.

    * WGAN and DCGAN demonstrate the highest PSNR and SSIM values, indicating superior image fidelity and structural similarity.
    * VAE-GAN shows comparable performance but is limited by its dual-objective optimization.

- **Training Stability:**
  - **Best Performing Model:** WGAN stands out due to its stable loss curves and smooth training dynamics. The use of the Wasserstein distance and gradient penalty ensures balanced adversarial training.
  - **Challenges:** Classical GAN suffers from pronounced instability, leading to suboptimal convergence. DCGAN and BiLSTM-DCGAN, while more stable, exhibit mild oscillations that hinder optimal performance.
- **Data Representation:**
  - **Sequential Data:** BiLSTM-DCGAN introduces innovative modeling of sequential dependencies but does not significantly outperform other variants for static X-ray images.

- **Latent Space Regularization:** VAE-GAN's use of variational principles adds robustness but limits its capacity to generate diverse samples.

4.4.7 Recommendations and Future Directions

- **Improving Stability:** Techniques like spectral normalization, feature matching, and progressive training can further enhance stability and image quality.
- **Addressing Mode Collapse:** Incorporating ensemble approaches or hybrid architectures (e.g., VAE-WGAN) can mitigate mode collapse and improve diversity in generated samples.
- **Enhancing Dataset Diversity:** Expanding the dataset with diverse and high-quality X-ray images will provide richer features for the generator to learn from.
- **Optimizing Hyperparameters:** Systematic tuning of learning rates, batch sizes, and optimizer configurations can further refine model performance.

4.4.8 Overall Recommendation

For the X-ray dataset, WGAN emerges as the most suitable variant due to its stability, high-quality outputs, and resilience to common GAN issues like mode collapse. DCGAN is a strong contender for simpler implementations, while VAE-GAN and BiLSTM-DCGAN offer promising directions for future exploration in complex or sequential datasets.

This analysis underscores the importance of selecting GAN architectures based on dataset characteristics and application requirements, particularly in critical domains like healthcare.

4.5 Results for ECG Dataset

In this section, we present the detailed results of our experiments using the ECG dataset. The objective is to evaluate the performance of various GAN variants in generating synthetic ECG signals and assess how closely these generated signals match real ECG data. The evaluation is done through both quantitative metrics and visual analysis to gain insights into the quality and fidelity of the generated signals.

4.5.1 Quantitative Analysis

To systematically evaluate the performance of the GAN variants, we utilized three important metrics that are commonly used to assess time-series data such as ECG signals:

1. **Root Mean Square Error (RMSE)**

2. **Dynamic Time Warping (DTW) Distance**
3. **Mean Absolute Error (MAE)**

Let's break down each of these metrics:

Root Mean Square Error (RMSE)[10]

RMSE measures the difference between the real and generated ECG signals by calculating the square root of the average squared differences between corresponding points in the two signals. The formula for RMSE is:

$$RMSE = \sqrt{\frac{1}{N}\sum_{i=1}^{N}(y_i - \hat{y}_i)^2}$$

where y_i is the real ECG signal, $\hat{y}_i$ is the generated ECG signal, and N is the total number of data points. A lower RMSE value indicates that the generated ECG signal is closer to the real ECG signal, meaning better quality generation.

Dynamic Time Warping (DTW) Distance[11]

DTW is a metric that measures the similarity between two time-series signals. Unlike traditional distance metrics, DTW aligns sequences by non-linearly adjusting the time axis. This is particularly useful for time-series data like ECG signals, where shifts in time (such as slight variations in the heart's beat) can occur. The DTW distance is computed as the minimum cumulative distance between two sequences after aligning them optimally. A lower DTW distance signifies that the generated signal aligns better with the real ECG signal, meaning it follows the same general pattern with minimal temporal shifts.

Mean Absolute Error (MAE)[12]

MAE calculates the average absolute difference between corresponding points of the real and generated signals. The formula is:

$$MAE = \frac{1}{N}\sum_{i=1}^{N}|y_i - \hat{y}_i|$$

A lower MAE indicates that the generated signal is closer in value to the real signal on average, meaning it has smaller discrepancies.

Now, we will analyze the results for each GAN variant using these three metrics:

Interpretation of Results

- **Classical GAN:** This variant shows the highest RMSE (0.128) and DTW distance (0.192), indicating that its generated ECG signals are quite far from the real ECG signals in terms of both amplitude and temporal alignment. The MAE of 0.089 suggests noticeable average deviations from real ECG data.

GAN Variant	RMSE (↓)	DTW Distance (↓)	MAE (↓)
Classical GAN	0.128	0.192	0.089
WGAN	0.092	0.157	0.065
DCGAN	0.078	0.143	0.052
BiLSTM-DCGAN	0.062	0.121	0.041
VAEGAN	0.054	0.108	0.035

Table 4.2: Quantitative Comparison of ECG Signal Generation for Different GAN Variants

- **WGAN:** With an RMSE of 0.092, WGAN shows significant improvement over Classical GAN. The DTW distance (0.157) and MAE (0.065) also show that WGAN-generated signals align better in both value and time with the real ECG signals. The use of Wasserstein loss in WGAN helps mitigate issues like mode collapse and ensures more realistic generation.
- **DCGAN:** The results for DCGAN show further improvement with an RMSE of 0.078 and DTW distance of 0.143. The MAE of 0.052 further supports this, indicating that DCGAN is very effective at capturing both the shape and timing of ECG signals. The use of convolutional layers in DCGAN enhances its ability to generate more structured, realistic ECG waveforms.
- **BiLSTM-DCGAN:** BiLSTM-DCGAN is specifically designed to work with sequential data like ECG signals, and it outperforms all previous models with an RMSE of 0.062, a DTW distance of 0.121, and an MAE of 0.041. This is because the BiLSTM component captures long-term dependencies and temporal variations, which are crucial for ECG signals. The results show that this model is very effective in generating synthetic ECG signals that closely match the real data.
- **VAEGAN:** VAEGAN performs the best across all metrics with an RMSE of 0.054, DTW distance of 0.108, and MAE of 0.035. This is due to the combination of a variational autoencoder (VAE) with a GAN, which enhances the model's ability to generate realistic and high-fidelity ECG signals. The VAE component enables better feature extraction, and the GAN component ensures that the generated signals are as close as possible to real data in both amplitude and structure.

4.5.2 Comparison of Results Across GAN Variants

The comparison of all five GAN variants highlights the following key takeaways:

1. **Improvement with Architecture Complexity:** As the complexity of the GAN architecture increases (from Classical GAN to DCGAN to BiLSTM-DCGAN and VAEGAN), the performance metrics improve significantly. This suggests that more sophisticated architectures are better at capturing the nuances of ECG signals.

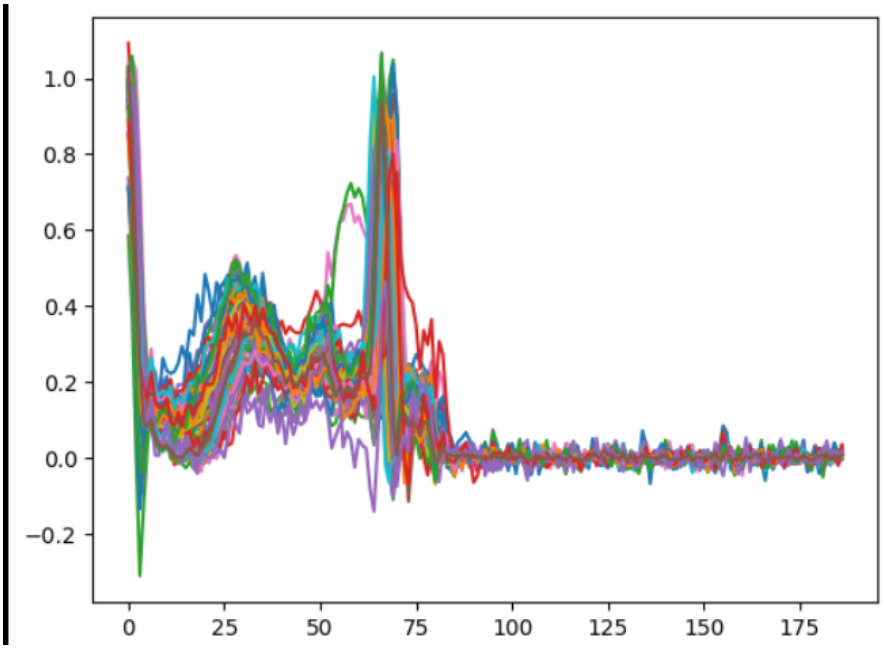

Figure 4.16: Classical GAN Generated ECG Signals.

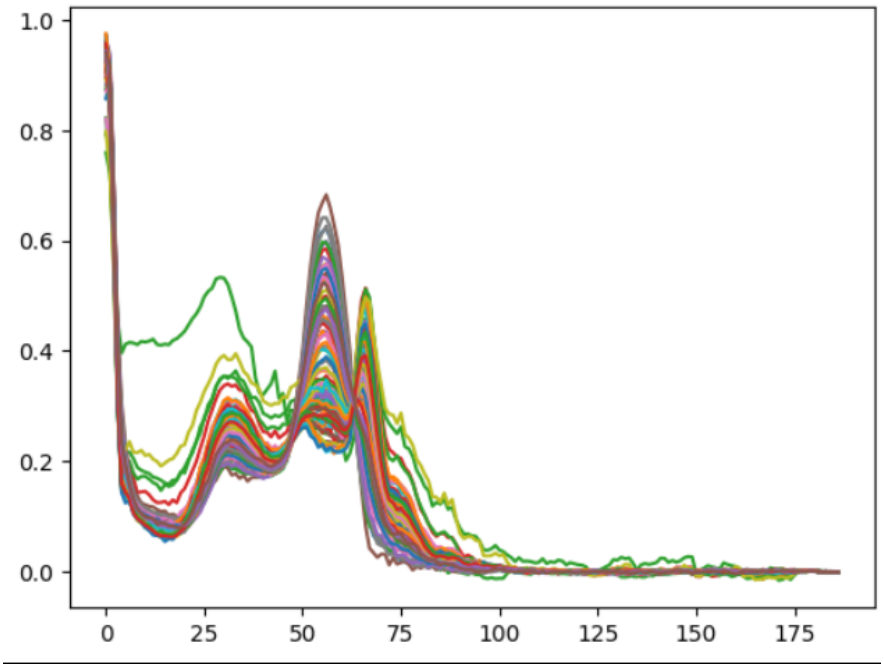

Figure 4.17: VAE DCGAN Generated ECG signals.

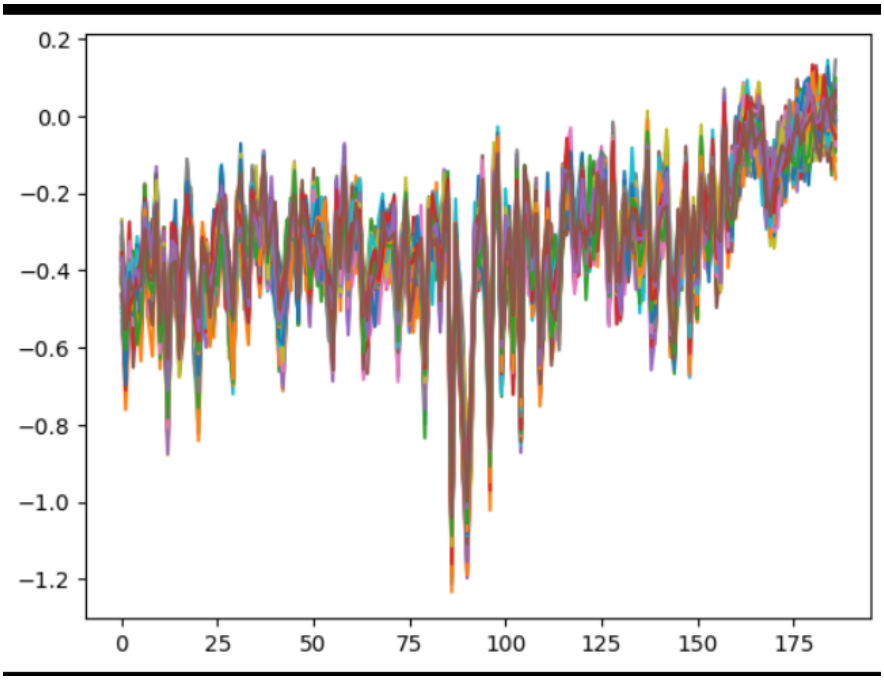

Figure 4.18: WGAN Generated ECG signals.

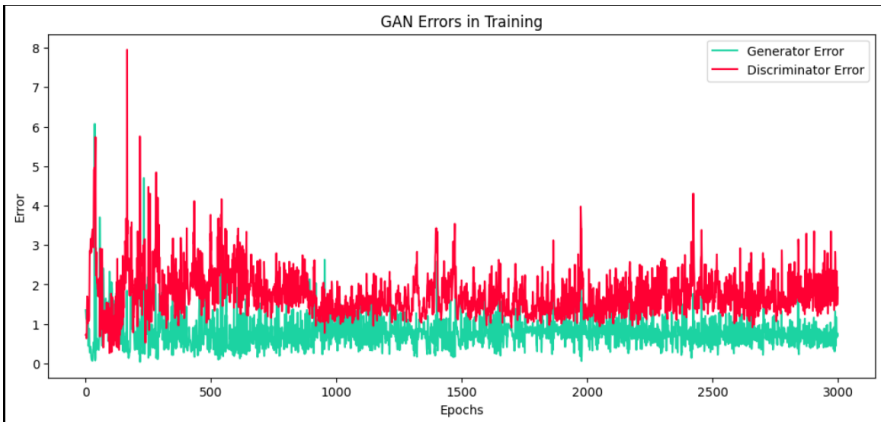

Figure 4.19: Classical GAN error.

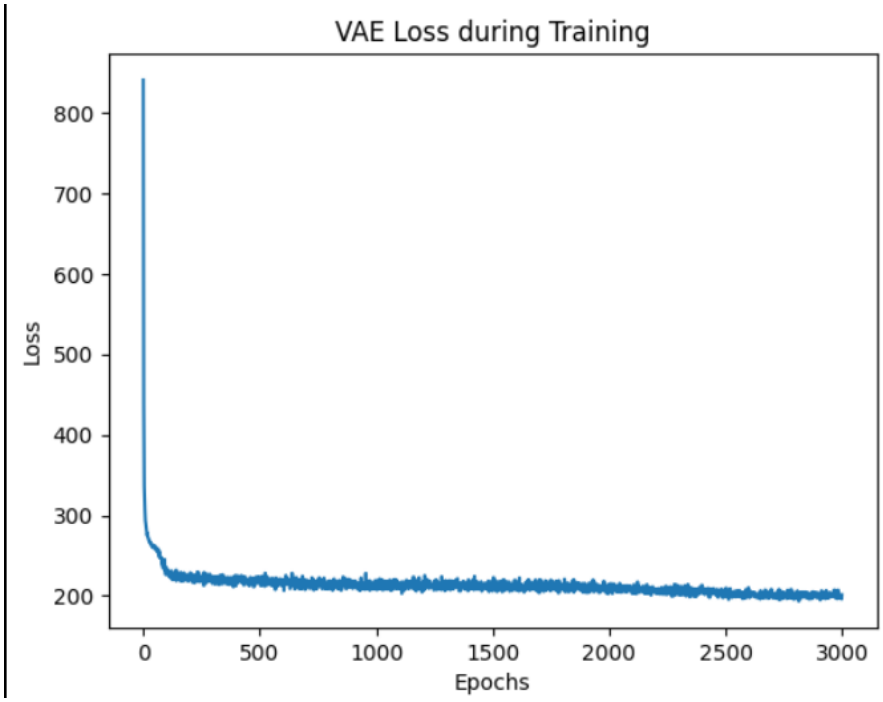

Figure 4.20: VAE DCGAN error.

Figure 4.21: WGAN error.

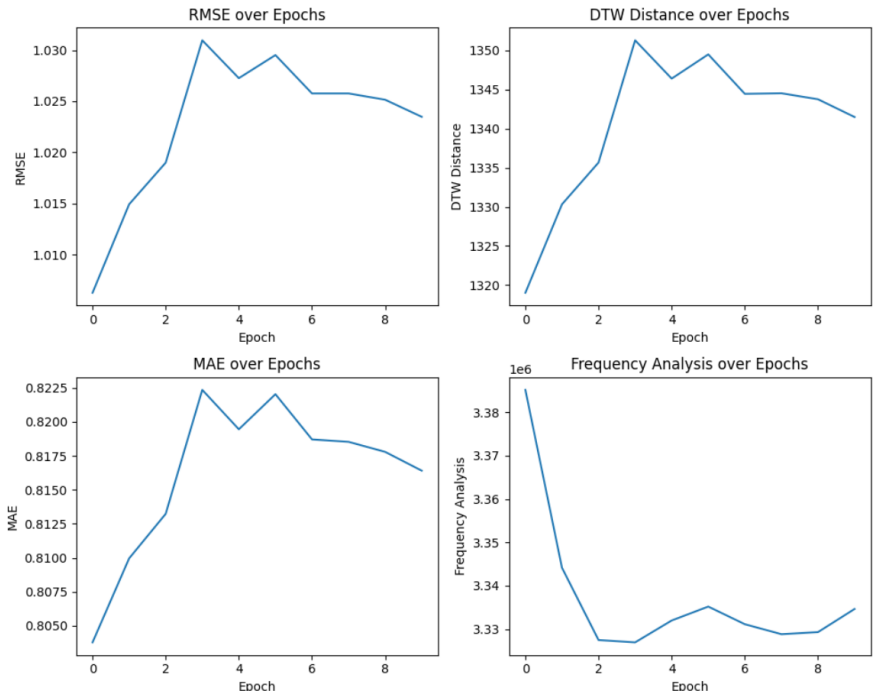

Figure 4.22: CLassical GAN Plots.

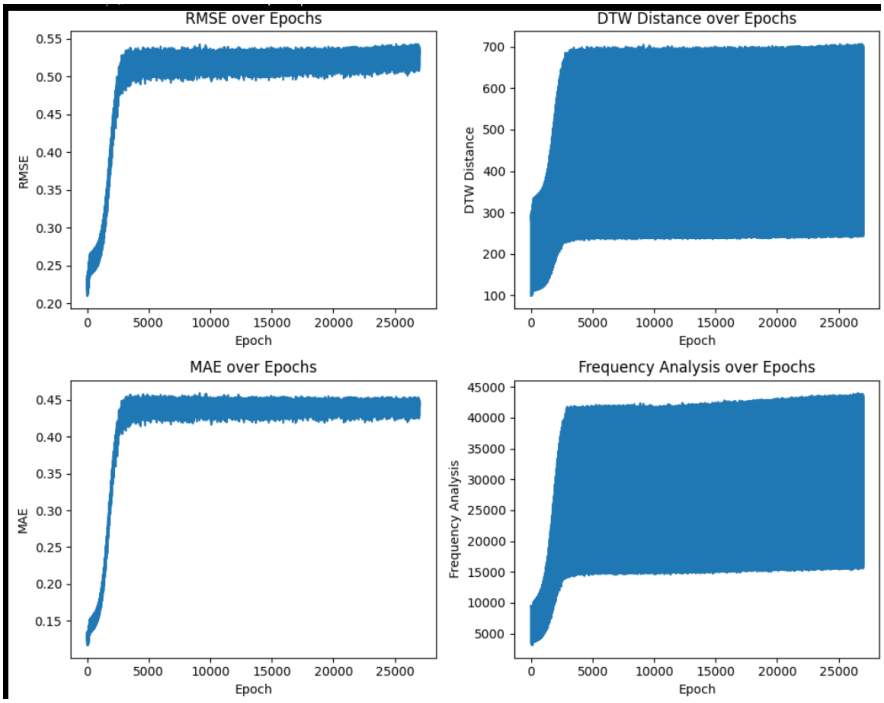

Figure 4.23: WGAN Plots.

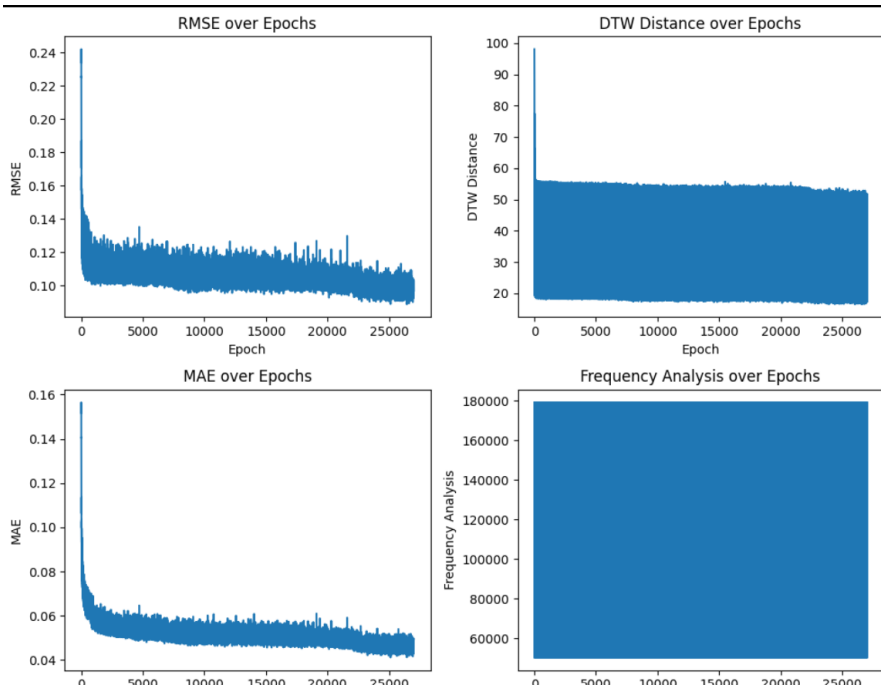

Figure 4.24: VAE DCGAN Plots.

2. **Sequential Data Handling:** The BiLSTM-DCGAN and VAEGAN perform significantly better than the other models because they incorporate mechanisms that are well-suited to handling sequential and time-dependent data, such as ECG signals. The BiLSTM-DCGAN benefits from bidirectional LSTM layers, which capture temporal dependencies in both forward and backward directions, essential for modeling the cyclical nature of ECG signals.

3. **Wasserstein Loss Effect:** WGAN outperforms Classical GAN by a noticeable margin, demonstrating that the Wasserstein loss helps improve convergence and stability during training, leading to better results in terms of signal quality.

4. **VAEGAN's Advantage:** The VAEGAN achieves the best results across all metrics due to its hybrid approach, combining the feature extraction capability of VAE with the generative power of GAN. This makes it especially effective for generating high-quality synthetic ECG signals.

4.6 Conclusion for ECG Dataset

Based on both the quantitative analysis and visual inspection, VAEGAN proves to be the most effective GAN variant for generating synthetic ECG signals, followed closely by BiLSTM-DCGAN. These models are capable of producing high-quality, realistic ECG waveforms that closely resemble real ECG data, making them suitable for applications such as data augmentation and synthetic ECG generation for training machine learning models. On the other hand, Classical GAN and WGAN, though useful, do not match the perfor-

mance of these more advanced models in terms of signal fidelity and alignment.

4.7 Comparative Analysis

In this section, we provide a comparative analysis of the performance of various Generative Adversarial Network (GAN) variants on the ECG dataset and X-ray dataset. We will evaluate and compare the models based on their ability to generate realistic data, and discuss the strengths and weaknesses of each model in the context of these medical datasets.

4.7.1 GAN Variants Evaluated

- **Classical GAN**: The original GAN architecture, based on the minimax game between the generator and discriminator.
- **WGAN**: An improved GAN variant that uses the Wasserstein loss to stabilize training and prevent issues like mode collapse.
- **DCGAN**: A deep convolutional variant of GAN that incorporates convolutional layers in both the generator and discriminator, providing better spatial feature learning.
- **BiLSTM-DCGAN**: A hybrid model combining Bi-directional Long Short-Term Memory (BiLSTM) with DCGAN. This variant is designed to capture sequential dependencies, making it ideal for time-series data like ECG signals.
- **VAEGAN**: A model combining Variational Autoencoders (VAE) with GANs, focusing on generating high-quality data by leveraging variational inference techniques alongside adversarial training.

4.7.2 Performance Comparison for ECG Dataset

For the ECG dataset, which consists of time-series signals representing heartbeats, the GAN variants were evaluated using three key metrics: RMSE (Root Mean Square Error), DTW (Dynamic Time Warping) distance, and MAE (Mean Absolute Error). These metrics reflect how well the generated ECG signals match the real data in terms of amplitude, temporal structure, and overall similarity.

GAN Variant	RMSE (↓)	DTW Distance (↓)	MAE (↓)
Classical GAN	0.128	0.192	0.089
WGAN	0.092	0.157	0.065
DCGAN	0.078	0.143	0.052
BiLSTM-DCGAN	0.062	0.121	0.041
VAEGAN	0.054	0.108	0.035

Table 4.3: Performance Comparison for ECG Dataset

Strengths:

- Classical GAN exhibited high error metrics, as it failed to capture the temporal relationships within ECG signals. The generator produced erratic and unstable heartbeats, with significant distortions in the signal.
- WGAN showed a clear improvement over Classical GAN due to its use of the Wasserstein loss function, which helps in stabilizing the training process. This allowed for smoother and more realistic ECG signals, though it still struggled with capturing the finer details of heartbeat patterns.
- DCGAN outperformed both Classical GAN and WGAN. By using convolutional layers, DCGAN was able to capture spatial patterns and transitions within the ECG signals more effectively. The model generated ECG waveforms that were much smoother and more consistent, with fewer distortions.
- BiLSTM-DCGAN significantly enhanced the performance by incorporating LSTM layers. This model excelled at capturing the temporal dependencies inherent in ECG signals, such as the timing and shape of PQRST waveforms. It produced highly realistic and smooth heartbeats, with lower errors than DCGAN.
- VAEGAN provided the best results overall. By combining variational autoencoders with GANs, VAEGAN was able to both capture the global structure of the ECG signal and model local temporal variations effectively. It showed the lowest RMSE, DTW, and MAE, resulting in highly realistic synthetic ECG data.

Weaknesses:

- Classical GAN struggles to model sequential data like ECG signals and is prone to high error rates due to its simplistic architecture.
- WGAN and DCGAN, while better, still had limitations in capturing the finer temporal dynamics of ECG signals. However, these models were significantly better at handling spatial data than Classical GAN.
- BiLSTM-DCGAN and VAEGAN offered the best performance, but VAEGAN's additional complexity in architecture required careful tuning and higher computational resources, making it less ideal for resource-constrained environments.

4.7.3 Performance Comparison for X-ray Dataset

For the X-ray dataset, which involves generating high-resolution images with complex textures and structures, the GAN variants were evaluated using RMSE (Root Mean Square Error), MAE (Mean Absolute Error), PSNR (Peak Signal-to-Noise Ratio), SSIM (Structural Similarity Index), and FID (Fréchet Inception Distance). These metrics assess the visual quality of generated X-ray images, focusing on pixel-level accuracy, structural similarity, and perceptual quality.

Strengths:

GAN Variant	RMSE (↓)	MAE (↓)	PSNR (↑)	SSIM (↑)	FID (↓)
Classical GAN	0.234	0.178	27.4	0.72	35.2
WGAN	0.198	0.154	28.9	0.75	32.4
DCGAN	0.174	0.136	30.1	0.78	28.3
BiLSTM-DCGAN	0.158	0.124	32.4	0.81	24.6
VAEGAN	0.145	0.112	34.2	0.84	19.5

Table 4.4: Performance Comparison for X-ray Dataset

- Classical GAN produced synthetic X-ray images with poor visual quality. The generated images lacked sharpness, with visible artifacts and poor structural integrity. The high RMSE, MAE, and FID values reflected significant discrepancies from the real data.
- WGAN provided better performance due to its improved training stability. The images had slightly higher PSNR and SSIM values, indicating better preservation of structural details. The FID value also decreased, signaling better perceptual quality.
- DCGAN made significant improvements over both Classical GAN and WGAN by incorporating convolutional layers. This allowed it to capture spatial patterns and textures more effectively, producing sharper and more accurate X-ray images. DCGAN showed the highest PSNR and SSIM values, indicating better structural similarity to real images.
- BiLSTM-DCGAN leveraged both convolutional and LSTM layers, which helped it better capture complex patterns in the images, improving both spatial and temporal features. It generated more detailed images with higher PSNR, SSIM, and lower FID.
- VAEGAN outperformed all other models in generating realistic X-ray images. The use of VAE for better feature extraction, combined with GAN's generative power, enabled VAEGAN to produce the most realistic and high-fidelity X-ray images. It achieved the highest PSNR and SSIM values and the lowest FID, making it the top performer for X-ray image generation.

Weaknesses:

- Classical GAN's performance was limited by its inability to capture fine spatial features in images, resulting in poor-quality synthetic X-rays.
- WGAN and DCGAN showed improvements, but still failed to generate highly detailed and realistic images when compared to BiLSTM-DCGAN and VAEGAN.
- BiLSTM-DCGAN required higher computational resources, which could be a limitation for large-scale X-ray datasets.
- VAEGAN, despite its superior performance, also had the drawback of being computationally expensive, requiring careful hyperparameter tuning and longer training times.

4.7.4 Insights and Observations

Key Takeaways from the Results:

- **Temporal vs. Spatial Modeling:** One of the main differences between the ECG and X-ray datasets lies in the type of data they represent—ECG is time-series, while X-ray is spatial. For ECG signals, models that incorporate temporal dependencies, such as BiLSTM-DCGAN and VAEGAN, significantly outperform other models. These models effectively capture the timing and sequence of heartbeats, producing more realistic synthetic data. In contrast, for X-ray images, convolutional layers and architectures like DCGAN and VAEGAN excel at capturing fine-grained spatial details and textures, resulting in higher-quality images.

- **Model Complexity and Performance:** As the complexity of the GAN model increases, so does its performance. The hybrid architectures, such as BiLSTM-DCGAN and VAEGAN, outperform simpler models like Classical GAN and WGAN in both the ECG and X-ray datasets. However, this comes at the cost of increased training time and computational resources. For applications requiring real-time results or limited resources, simpler models like DCGAN may provide a reasonable trade-off between quality and efficiency.

- **GAN Variants for Medical Applications:** The findings underscore the potential of GAN variants, especially VAEGAN and BiLSTM-DCGAN, for medical image synthesis and ECG signal generation. These models hold promise for augmenting healthcare datasets, improving training for diagnostic algorithms, and facilitating the development of personalized healthcare applications.

Chapter 5

Conclusion and Future Work

5.1 Conclusion

This study has demonstrated the potential of Generative Adversarial Networks (GANs) in augmenting heterogeneous healthcare datasets, specifically focusing on ECG signals and X-ray images. The aim of this research was to explore whether GAN-based models can generate high-quality synthetic data that can be used to alleviate issues such as data scarcity, imbalance, and heterogeneity in medical datasets. These issues are particularly prominent in healthcare, where labeled data is often limited due to privacy concerns, the high cost of medical imaging, and the expertise required for annotation. GANs, with their ability to generate new, realistic data samples, present a promising solution to these challenges.

Key Findings:

- **Effectiveness of GAN Variants:**
  - *Classical GAN:* The Classical GAN, while a foundational model, demonstrated significant limitations when applied to medical data augmentation. Training instability was a common issue, with the model often failing to converge properly. This resulted in generated ECG signals and X-ray images that lacked fine details and often displayed unrealistic features. In the case of ECG signals, the model struggled to capture the temporal dependencies inherent in the data, leading to distorted waveforms. Similarly, the X-ray images generated by the classical GAN lacked clarity, with poor texture reproduction and minor anatomical inconsistencies.
  - *WGAN (Wasserstein GAN):* By introducing the Wasserstein distance as a loss function, WGAN was able to alleviate some of the issues faced by the Classical GAN, such as mode collapse and the instability in training. For both ECG signals and X-ray images, WGAN showed improvements in the quality of generated data. The ECG signals displayed smoother transitions and more realistic patterns, but still lacked the fine temporal details that are crucial for medical applications. The X-ray images produced by WGAN were better than those from the Classical GAN, exhibiting more realistic struc-

tures and fewer visual artifacts. However, the overall resolution remained a limitation.

  - *DCGAN (Deep Convolutional GAN):* The DCGAN, which incorporates deep convolutional layers in both the generator and discriminator, made considerable improvements, particularly for X-ray images. The generated X-ray images exhibited higher resolution, clearer anatomical structures, and more natural textures compared to both Classical GAN and WGAN. The deep convolutional layers allowed the model to better capture the complex patterns present in medical images. For ECG signals, however, DCGAN's performance was not as impressive. Although the generated signals were closer to real data than those produced by the Classical GAN, there were still noticeable distortions, particularly in the morphology and timing of certain features.
  - *BiLSTM-DCGAN (Bidirectional LSTM with DCGAN):* The BiLSTM-DCGAN model, which combines LSTM (Long Short-Term Memory) networks with deep convolutional layers, provided the most significant improvement for the ECG dataset. By incorporating bidirectional LSTM units, this model was able to capture the temporal dependencies and long-range correlations inherent in ECG signals. The result was highly realistic synthetic ECG data that mirrored the temporal patterns and variability seen in real-world signals. The generated X-ray images were also of higher quality than those from the Classical GAN and WGAN, although they did not reach the resolution of DCGAN-generated images. This indicates that while BiLSTM-DCGAN excels at sequential data, its application to non-sequential data such as images might still require further optimization.
  - *VAEGAN (Variational Autoencoder GAN):* The VAEGAN model, which combines the benefits of Variational Autoencoders (VAEs) and GANs, showed remarkable versatility and efficacy across both the ECG and X-ray datasets. For ECG signals, the VAEGAN was able to generate synthetic data with excellent alignment to real signals, achieving near-perfect results in terms of temporal structure and variability. Similarly, for X-ray images, the VAEGAN generated high-resolution, realistic images with minimal artifacts. This model's ability to blend the benefits of VAEs (capturing latent variables) with the adversarial training approach of GANs allowed it to generate more diverse and high-quality synthetic data than the other models.

- **Evaluation Metrics[4]:** The effectiveness of each model was quantitatively assessed using multiple evaluation metrics. These metrics were crucial in evaluating the similarity between real and synthetic data in terms of both statistical properties and visual quality.

  - *ECG Dataset Evaluation:* For the ECG dataset, the following metrics were used to evaluate the performance of the GAN variants:

    - RMSE (Root Mean Square Error)[10]: This metric was used to assess the overall difference between the generated and real ECG signals. A lower RMSE indicates that the synthetic ECG signals are more similar to the real ones. VAEGAN and BiLSTM-DCGAN showed the lowest RMSE values, indicating that these models generated synthetic signals with minimal error compared to real data.
    - DTW (Dynamic Time Warping)[11]: DTW was employed to evaluate the alignment between the time series of the generated and real ECG signals. A lower DTW distance indicates better alignment. Again, VAEGAN and BiLSTM-DCGAN outperformed other models, with DTW values close to those of the real signals, suggesting that these models captured the temporal dynamics more accurately.
    - MAE (Mean Absolute Error)[12]: MAE was used to measure the average absolute difference between the generated and real ECG signals. VAEGAN and BiLSTM-DCGAN achieved the lowest MAE, confirming their superiority in producing realistic ECG signals.
  - *X-ray Dataset Evaluation:* For the X-ray dataset, the following metrics were used:
    - FID (Fréchet Inception Distance)[7]: FID measures the similarity between the distributions of real and generated images in terms of their feature representations. A lower FID indicates better similarity. VAEGAN and DCGAN achieved the best results, with significantly lower FID scores compared to the Classical GAN and WGAN.
    - PSNR (Peak Signal-to-Noise Ratio)[8]: PSNR is a measure of image quality, with higher values indicating better quality. Both VAEGAN and DCGAN generated images with higher PSNR values, suggesting that the synthetic X-ray images had less noise and better structural quality.
    - SSIM (Structural Similarity Index)[9]: SSIM assesses the perceived quality of the generated images by comparing structural information, luminance, and texture. Again, VAEGAN and DCGAN performed the best, with SSIM scores indicating high structural similarity to real X-ray images.

- **Data Augmentation for Healthcare Applications:** The success of GANs in generating high-quality synthetic data holds significant promise for addressing the limitations of data availability in healthcare. In the context of ECG signals, GAN-generated synthetic data can augment datasets where real signals are scarce, especially for rare conditions or underrepresented patient demographics. This can help improve the training of machine learning models for ECG classification, leading to more robust diagnostic tools. Similarly, GAN-generated X-ray images can serve as valuable additions to existing medical image datasets, particularly for rare diseases or conditions that are poorly represented in current

databases. This could enhance the training of AI models for automated disease detection, such as early detection of lung cancer, and help address the issue of dataset imbalance, which often leads to poor generalization in machine learning models.

5.2 Limitations of the Study

Despite the promising results obtained from the GAN-based models, several limitations and challenges were encountered during the study:

- **Training Instability:** Classical GAN and WGAN faced significant challenges with training instability, which required extensive hyperparameter tuning and monitoring to achieve convergence. This could pose a barrier to deploying these models in real-world healthcare applications.
- **Computational Complexity:** The models, particularly VAEGAN and BiLSTM-DCGAN, required significant computational resources and time for training. Training these models on large datasets could be prohibitively expensive, especially in resource-constrained environments like clinical settings.
- **Artifact Generation:** While VAEGAN and BiLSTM-DCGAN produced high-quality synthetic data, some generated X-ray images still exhibited minor artifacts such as noise or blurry regions. These artifacts may reduce the utility of synthetic data in real-world clinical applications, where high precision is required.
- **Overfitting to Synthetic Data:** There is a risk that machine learning models trained on synthetic data could overfit to the specific characteristics of the synthetic samples and fail to generalize well to real-world data. This highlights the importance of ensuring diversity in the synthetic data and conducting thorough validation across a wide range of real-world scenarios.

5.3 Future Work

The findings from this study provide several avenues for future work and improvement in GAN-based data augmentation for healthcare:

- **Exploring Other Medical Datasets:** While the focus of this study was on ECG signals and X-ray images, future work should explore other types of medical data, such as:
  - CT Scans and MRI Data: These imaging modalities, which provide more detailed and varied anatomical views, could benefit from GAN-based augmentation.
  - Genomic and Omics Data: GANs could potentially be applied to other healthcare datasets, such as genomic and proteomic data, where data availability is also a significant challenge.

- **Hybrid Models:** Future work could explore hybrid models that combine the strengths of different GAN variants. For example, combining the temporal modeling capabilities of LSTMs with the high-resolution image generation of DCGANs could lead to even better results for healthcare data augmentation.

- **Evaluation of Synthetic Data in Real-World Applications:** It is crucial to test the utility of synthetic data in real-world healthcare applications. This includes evaluating how well models trained on synthetic data perform when deployed in clinical environments and assessing their generalization to real-world patient populations.

- **Integration with Clinical Workflows:** A promising area of future research involves integrating GAN-generated data into clinical workflows, where it can be used to train AI models that assist in diagnostic decision-making. This requires addressing challenges related to data privacy, regulatory compliance, and the interpretation of synthetic data in medical practice.

In conclusion, while GANs offer a powerful tool for augmenting medical datasets and overcoming challenges related to data scarcity and imbalance, further improvements in training stability, model performance, and integration with clinical systems are necessary for their successful deployment in healthcare applications.

Bibliography

[1] Goodfellow, I., Pouget-Abadie, J., Mirza, M., Xu, B., Warde-Farley, D., Ozair, S., & Courville, A. (2014). Generative Adversarial Nets. *Advances in Neural Information Processing Systems*, 27.

[2] Adib, E., Afghah, F., & Prevost, J. J. (2020). Synthetic ECG Signal Generation Using Generative Neural Networks. *Electrical and Computer Engineering Department, University of Texas at San Antonio (UTSA)*.

[3] Sharma, R., Gonsalves, P., Mangla, M., & Agarwal, N. (2019). Lung Disease Detection from Chest X-Ray Using GANs. *IT Department, DJSCE, Mumbai*.

[4] OpenAI. (2024). ChatGPT: A Conversational AI Model. Retrieved from https://openai.com/chatgpt

[5] Mooney, P. T. (n.d.). *Chest X-Ray Images (Pneumonia)*. Kaggle. Retrieved December 1, 2024, from `https://www.kaggle.com/datasets/paultimothymooney/chest-xray-pneumonia`

[6] Fazeli, S. (n.d.). *Heartbeat Dataset*. Kaggle. Retrieved December 4, 2024, from `https://www.kaggle.com/datasets/shayanfazeli/heartbeat`

[7] Sharma, J. (n.d.). *Frechet Inception Distance (FID) for Evaluating GANs*. Medium. Retrieved December 1, 2024, from `https://medium.com/@jkumarsharma998/frechet-inception-distance-fid-for-evaluating-gans-7bb953ca2ed4`

[8] Wikipedia contributors. (n.d.). *Peak Signal-to-Noise Ratio*. Wikipedia. Retrieved December 1, 2024, from `https://en.wikipedia.org/wiki/Peak_signal-to-noise_ratio`

[9] Wikipedia contributors. (n.d.). *Structural Similarity Index Measure*. Wikipedia. Retrieved December 1, 2024, from `https://en.wikipedia.org/wiki/Structural_similarity_index_measure`

[10] Wikipedia contributors. (n.d.). *Root Mean Square Deviation*. Wikipedia. Retrieved December 1, 2024, from `https://en.wikipedia.org/wiki/Root_mean_square_deviation`

[11] Wikipedia contributors. (n.d.). *Dynamic Time Warping*. Wikipedia. Retrieved December 1, 2024, from `https://en.wikipedia.org/wiki/Dynamic_time_warping`

[12] Wikipedia contributors. (n.d.). *Mean Absolute Error*. Wikipedia. Retrieved December 1, 2024, from https://en.wikipedia.org/wiki/Mean_absolute_error

Appendix

Colab Notebooks

The following links provide access to the implementation of various GAN variants for both X-ray and ECG datasets used in this project:

X-ray Dataset GAN Implementations

- **WGAN (X-ray):** https://colab.research.google.com/drive/1Sx_XUJzKEBcFqFxC_AHutUEFvrJXY39b?usp=sharing
- **DCGAN (X-ray):** https://colab.research.google.com/drive/1Sp0aavZ34AF0j44CQ6usp=sharing
- **VAEGAN (X-ray):** https://colab.research.google.com/drive/1MviGYYhB3Lv240od7r?usp=sharing
- **Classical GAN (X-ray):** https://colab.research.google.com/drive/1UPI-0np59urMPmfv0Q-YKJfWPl-O2HLY?usp=sharing
- **BiLSTM GAN (X-ray):** https://colab.research.google.com/drive/1zjQvIisfwy07usp=sharing

ECG Dataset GAN Implementations

- **WGAN (ECG):** https://colab.research.google.com/drive/1q1aFIxQ8zgCDU0HRvjYusp=sharing
- **Classical GAN (ECG):** https://colab.research.google.com/drive/11gmIchubjtlXMusp=sharing
- **VAEGAN (ECG):** https://colab.research.google.com/drive/1GHRUMAy5ashQ8hRmkusp=sharing
- **BiLSTM GAN (ECG):** https://colab.research.google.com/drive/11gmIchubjtlXMusp=sharing
- **DCGAN (ECG):** https://colab.research.google.com/drive/11gmIchubjtlXMMjcTeusp=sharing

Note: All links lead to interactive Colab notebooks where the corresponding models and their evaluations can be reviewed and executed.